The Astronomy And Astrophysics Review Manuscript-Nr.
(will be inserted by hand later)

The emission line spectrum of active galactic nuclei and the unifying scheme

M.P. Véron-Cetty and P. Véron

Observatoire de Haute Provence, CNRS, F-04870 Saint-Michel l'Observatoire, France

Received: 16 november 1999

Summary. Recent papers dealing with the most controversial aspects of AGNs are reviewed. They suggest interesting conclusions: all Seyferts can be described by a single parameter, the X-ray column density; radio loud AGNs may host a rapidly spinning black hole and radio quiet AGNs a slowly spinning black hole; high-ionization AGNs (Seyfert galaxies and QSOs) contain an optically thick, geometrically thin accretion disk, while low-ionization AGNs (Liners) contain an optically thin, geometrically thick accretion disk; a number of blazars have been classified as BLLs on the basis of insufficient data; most objects with weak broad emission lines are in fact HPQs; many objects have been called Liners although they are not AGNs but rather the result of stellar activity; type 2 QSOs exist, but are quite inconspicuous if radio quiet.

TABLE OF CONTENTS

Correspondence to: P. Véron, veron@obs-hp.fr

1. INTRODUCTION

Seyfert 1s are normal spiral or E galaxies with a compact, starlike nucleus and a nuclear emission line spectrum characterized by broad (a few thousands km s^{-1}) permitted lines and narrow (a few hundreds km s^{-1}) high excitation lines. Seyfert 2s have a narrow emission line spectrum like the Seyfert 1s, but they are lacking both the compact nucleus and the broad emission lines. Quasars (or QSOs) are high luminosity Seyfert 1 nuclei ($M_B < -24$; throughout this paper, we use H_o=50 km s^{-1} Mpc^{-1} and q_o=0.5); their luminosity is so high that the host galaxy is difficult to detect. Seyferts and QSOs contain a compact nuclear continuum source ionizing a broad line region, surrounded by an optically thick torus of dust. Depending on the orientation of this torus with respect to the line of sight, the central object is seen or hidden; when it is hidden, we see only the narrow, extended emission line region; the galaxy is a Seyfert 2. The major breakthrough in understanding the connection between Seyfert 1s and 2s was the discovery by Antonucci & Miller (1985) of a "hidden" broad line region (BLR) in the Seyfert 2 NGC 1068.

Many spiral galaxies contain a starburst in their central region. Spectra of narrow line Seyferts and starbursts are easily distinguished by their main emission line ratios. But diagnostic diagrams built with these emission line ratios reveal a third type of emission line spectra called Liners (Low Ionization Nuclear

Emission line Region). Some of these objects are most probably low luminosity Active Galactic Nuclei (AGNs); others must be related to the cooling flow phenomenon occuring in clusters of galaxies or are produced in the collision and merging of gas rich galaxies.

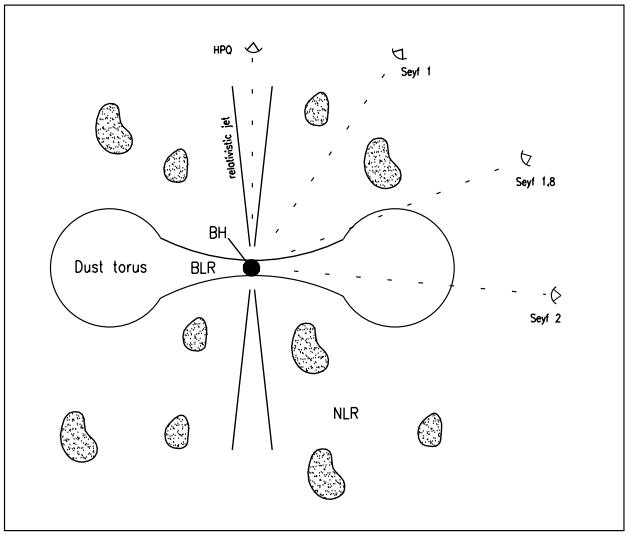

Fig. 1. Schematic diagram of FR II active nuclei showing how the appearance can change from NLRG (Seyfert 2) to BLRG (Seyfert 1) to HPQ with changing viewing angle.

Seyferts and QSOs can be radio loud or radio quiet. Radio loud objects are always hosted by an E galaxy. Most radio galaxies have a double lobe structure; the high radio luminosity sources have edge-brightened lobes; they are called FR II radio sources (for Fanaroff-Riley type II). The low luminosity sources are called FR Is. FR II radio galaxies have the nuclear emission line spectrum of Seyferts; when they have broad emission lines they are called Broad Line Radio Galaxies (BLRGs); when they have the emission line spectrum of a Seyfert 2, they are called Narrow Line Radio Galaxies (NLRGs). All radio quasars have a FR II morphology. FR Is have a weak low excitation emission line spectrum, similar to Liners or no detectable emission at all.

The lobes of radio galaxies (FR Is and FR IIs) are powered by a relativistic jet; when the angle between the jet axis and the line of sight is small, the jet is Doppler boosted by a large factor and the whole spectrum (from radio to γ-ray) is dominated by a compact, highly polarized, highly variable, superluminal, almost featureless continuum. These objects are called blazars; they are divided into two subclasses: the Highly Polarized Quasars (HPQs) which show broad emission lines, and the BL Lacertae objects (BLLs) with no or weak broad emission lines. The parent population of the HPQs is made of the FR IIs, while the parent population of the BLLs is made of the FR Is. Fig. 1 is a schematic diagram of an FR II galaxy showing how the appearance changes with the viewing angle.

The most popular explanation for the AGN powerhouse involves accretion of gas onto a supermassive, perhaps spinning black hole (BH). Different regimes of accretion have been invoked to constitute the basis of a unified picture of AGNs. The predictions of the theory are that rotationally supported thin disks would form at lower accretion rates ($\dot{M}<\dot{M}_{\rm Edd}$), while supercritical ($\dot{M}\geq\dot{M}_{\rm Edd}$) accretion flows are expected to form thick disks supported by radiation pressure. A very subcritical flow may not be able to cool and, instead of forming a thin disk, it puffs up giving rise to an ion torus supported by gas, rather than radiation, pressure (Abramowicz et al. 1987; Narayan et al. 1999).

This is, very schematically, the generally accepted Unified Scheme of AGNs.

A number of reviews have been published in recent years dealing with various aspects of this topic: a brief history of AGNs (Shields 1999), emission line regions (Osterbrock & Mathews 1986), continuum radiation (Bregman 1990), ultraviolet and optical continuum emission (Koratkar & Blaes 1999), emission lines (Netzer 1990; Korista 1999), BALQSOs (Weymann 1997), X-ray properties (Mushotzky et al. 1993; Mushotzky 1997), high-energy radiation (Sikora 1994), variability (Wallinder et al. 1992; Wagner & Witzel 1995; Ulrich et al. 1997), parsec-scale jets (Zensus 1997), structure (Miley 1980) and polarization (Saikia & Salter 1988) of extended extragalactic radio sources, Liners (Heckman 1987; Filippenko 1996; Ho 1998), BLLs (Valtaoja et al. 1992; Kollgaard 1994), blazars (Takalo 1994), accretion disks (Begelman 1985; Abramowicz et al. 1987; Collin-Souffrin 1994; Narayan et al. 1999) and black holes in galactic nuclei (Kormendy & Richstone 1995; Richstone et al. 1998), the torus model (Antonucci 1996), the unified scheme (Lawrence 1987; Antonucci 1993; Urry & Padovani 1995), physical processes in AGNs (Blandford 1990), ionized gas in E galaxies (Goudfrooij 1999), luminous infrared galaxies (Sanders & Mirabel 1996), interacting galaxies (Barnes & Hernquist 1992),...

In the following, we review recent work which has brought some light on several as yet unanswered questions: the nature of Liners, the distinction between HPQs and BLLs, the basic differences between high- and low-ionization radio galaxies and between radio loud and radio quiet AGNs, the source of energy powering ULIGs, the existence of type 2 QSOs, ...

2. SEYFERT GALAXIES AND QSOs

2.1. Seyfert 1 and Seyfert 2 galaxies

2.1.1. The emission line spectrum of Seyfert 2 galaxies

Seyfert 2s are characterized by a spectrum having both strong high- and low-ionization emission lines. The emission line spectra of Seyfert 2s are not accurately described by simple photoionization models of single clouds.

To explain both high and low ionization lines, the narrow-line region (NLR) must be composed of a mixture of dust-free, metal depleted ($\sim$0.5 solar, except for nitrogen which may be enhanced relative to the solar value by a factor 2) clouds with a radius-independent range in densities (10^2 to 10^5 cm^{-3}) distributed over a range of distances from the nucleus. To encompass the observed range of line intensities relative to Hβ, it is necessary to vary the spectral energy

distribution incident on the clouds by adding a varying contribution of a hot blackbody (T$\sim$2-6 10^5 K) to a steep X-ray power-law spanning 13.6 to 100 keV (Komossa & Schulz 1997; Ferguson et al. 1997a).

Véron & Véron-Cetty (1986) found that the width of the narrow emission lines correlates with the Hubble types in Seyferts, earlier types having broader lines; they suggested that these line widths could correlate with the mass of the bulges. This was confirmed by Nelson & Whittle (1996) who found a correlation between line width and nuclear stellar velocity dispersion suggesting that gravitational motion plays an important role in the narrow line velocity field.

The redshifts obtained from the nuclear emission lines in Seyferts are on average smaller than the systemic velocities by about 60 km s^{-1}, with differences reaching 250 km s^{-1} (Mirabel & Wilson 1984).

2.1.2. The emission line spectrum of Seyfert 1 galaxies and QSOs

In addition to a narrow-line emission spectrum, Seyfert 1s have broad permitted lines (H I, He I $\lambda\lambda$5876,6678,7065, He II λ4686 and Fe II in the visible domain).

The narrow-line spectra of Seyfert 1s are very similar to those of Seyfert 2s; there are however significant differences, most notably much stronger high-ionization lines ([Fe VII]λ6087, [Fe X]λ6375, [Fe XI]λ7892) in some Seyfert 1s (Cohen 1983; Erkens et al. 1997; Schmitt 1998). Ferguson et al. (1997b) showed that these "coronal lines" form just outside the BLR, in clouds with electron temperatures T$\sim$ 12 000-150 000 K and densities of 10^2-$10^{8.5}$ cm^{-3}.

There seems to be an anticorrelation between R_{5007}, the ratio of the intensities of the broad Hβ component to the [O III]λ5007 line and the broad Hβ component luminosity or the continuum luminosity, *i.e.* bright QSOs have relatively weak narrow lines (since in the NLR R_{5007} $\sim$0.1, the measurement of R_{5007} is a measurement of the ratio of the broad to the narrow Hβ component fluxes). There are however probably no "pure" Seyfert 1s, *i.e.* bare BLRs without surrounding NLRs; the objects which come closest are the Seyfert Mark 231, in which the only identified narrow line is [O II]λ3727 and the QSO 3C 273 (Cohen 1983).

The decrease in the relative amount of narrow-line emission with luminosity suggests either that the ionizing flux to the narrow-line region is proportionately smaller in objects with a high-luminosity broad-line component, or else that there is proportionately less low-density gas in the higher luminosity Seyferts (Cohen 1983).

The broad emission lines observed in AGNs have a FWHM which is typically in the range 5 000-10 000 km s^{-1} and show different kinds of profiles that usually are not Gaussian or even symmetrical (Stirpe 1991; Corbin 1995). The half-width at zero intensity of Hβ can be extremely large, reaching 35 000 km s^{-1} in the case of PG 0052+251 (Boroson & Green 1992). Crenshaw (1986) showed that the Hβ/Hα and He I λ5876/Hβ ratios increase from the core to the wings of the lines, indicating that the broad-line region is not a thin spherical shell.

Woltjer (1959) was the first to suggest that the width of the lines could be due to fast motions in the gravitational field of a massive nucleus. Assuming the line-emitting matter is gravitationally bound, and hence has a near-Keplerian velocity dispersion (indicated by the line width), it is possible to estimate the central mass. The main problem in estimating the mass from the emission line data is to obtain a reliable estimate of the size of the BLR; this size can be measured by reverberation mapping. Both the continuum and the broad emission line fluxes are variable in Seyfert 1s and QSOs; the time lags between the emission line and the continuum light curves can be interpreted in terms of the delayed response of the spatially extended BLR to the ionizing continuum source. These observations have established that Seyfert 1 BLRs have sizes of the order of a few light-days to light-months ($\sim$100 light-days). The BLR size of these objects is consistent with the hypothesis that the BLR size grows as $L^{0.5}$ as expected if the shape of the ionizing continuum in AGNs is independent of the luminosity L, and that all AGNs are characterized by the same ionization parameter and BLR gas density (Kaspi et al. 1996; Wandel 1997). The Hβ FWHM correlates with the Hβ luminosity, probably reflecting a scaling of the central mass with the luminosity (Miller et al. 1992). Whether or not the broad emission line widths actually reflect virial motions is still somewhat problematic; if however this is the case, the BLR provides a definitive demonstration of the existence of supermassive BHs. An estimate has been made by the reverberation mapping method of the BH mass in 19 Seyfert 1s; these masses range from 0.4 to 40 10^7 $M_\odot$ (Wandel et al. 1999). The average black-hole-to-bulge mass ratio is 0.0003 for AGNs (Wandel 1999) while it is 20 times larger for bright QSOs (Laor 1998).

Despite intensive studies, the BLR is still poorly understood.

It is now widely believed that accretion of gas into a central supermassive BH lies at the heart of the phenomenon; the accretion flow takes the form of a geometrically thin disk which is the source of the X-ray, UV and optical continuum emission which ionizes circumnuclear gas in both the broad-line and narrow-line regions; the BLR is made of an assembly of small clouds, photoionized by the continuum emission of the disk; this results from the fact that the "effective" volume giving rise to the emission is much smaller than L^3, where L is the typical size of the emitting region deduced from the variability time-scale and the ionization parameter. However, these requirements can also be fulfilled if the lines are emitted by a continuous medium whose thickness is much smaller than its lateral dimension, for instance a thin disk or the atmosphere of a disk. Assuming that the velocity is Keplerian, FWHM of $\sim$ 5 000-10 000 km s^{-1} implies that this material is located at distances of about 10^3-10^4 R_S from the center (where R_S is the Schwarzschild radius $2GM/c^2$); if the disk is heated by the down scattered part of the non-thermal continuum observed in AGNs, the physical parameters of the optically thin region satisfy the requirements of photoionization models for the line emission (Collin-Souffrin 1987). In these conditions, the low ionization lines (Balmer lines, Fe II lines, Mg II) can be emitted mostly by the accretion disk, but not the high-ionization lines (Lyα, C IV, C III]) which are likely emitted by a dilute outflowing medium; this model yields BH masses in the range 10^7-10^9 $M_\odot$ for a sample of six Seyfert 1s (Rokaki et al. 1992). In NGC 5548, the emission lines are variable, but are best explained by the superposition of an emission line cloud with variable lines and another which shows no variability;

the non variable cloud may not be radiatively heated; it is in collisional equilibrium with a temperature $\sim 10^4$ K; its emission spectrum is dominated by Balmer lines and Fe II emission (Dumont et al. 1998).

The traditional QSO BLR consists of two components: one with $\sim$ 2 000 km s^{-1} FWHM, the intermediate line region (ILR), and another very broad component of width $>$ 7 000 km s^{-1} FWHM, the very broad line region (VBLR); the spectra of the ILR and VBLR are very different; the high-ionization lines are relatively stronger in the VBLR (Brotherton et al. 1994). The ILR and VBLR are probably identical with the low- and high-ionization line regions identified by Rokaki et al. (1992).

A highly significant correlation has been found for radio loud QSOs between the line widths (FWHM) of broad Hβ lines and the relative strength of the compact radio nucleus; this is expected in beaming models if the predominant motion in the line emitting gas is confined to a disk lying perpendicular to the radio axis which is the case if the ILR is in the thin disk (Wills & Browne 1986; Boroson & Green 1992).

There is an anticorrelation of the EW of broad lines (C IV λ1550, C III]λ1909 and Mg II λ2798) with the continuum luminosity; these correlations are substantially stronger for the radio selected sample than for the radio quiet sample (Steidel & Sargent 1991; Puchnarewicz et al. 1997). This is the so-called "Baldwin effect". There is no evidence for a Baldwin effect in the broad Hα or Hβ component (Miller et al. 1992).

A small number of AGNs, mainly but not exclusively radio loud, have been found to have double-peaked line profiles which could originate in Keplerian thin disks; they have a mean FWHM of $\sim$ 12 500 km s^{-1}; their spectra are characterized by large [O I]/[O III] ratios, *i.e.* they are Liner-like (Eracleous & Halpern 1994; Halpern & Eracleous 1994; Storchi-Bergmann et al. 1995; Rodriguez-Ardila et al. 1996). In one of these objects, Arp 102B, UV spectra show broad Mg II present with nearly the same profile as the Balmer lines, but there is little, if any, C III], C IV or Ly α emission corresponding to the displaced Balmer-line peaks, demonstrating the need to invoke different locations and different physical conditions for double-peaked and single-peaked line components in the same object. The double-peaked component could be the low temperature, collisionally excited region postulated by Dumont et al. (1998).

H_2O megamasers have been looked for in a number of nearby galaxies; they have been detected in 11 Seyfert 2s, never in Seyfert 1s; this lack of detection in Seyfert 1s indicates either that they do not have molecular gas in their nuclei with physical conditions appropriate to produce 1.3 cm H_2O masers, or that masers are beamed away from Earth, in the plane of the obscuring molecular torus; the first possibility would violate the unified scheme (Braatz et al. 1997). Kartje et al. (1999) suggested that the maser emission regions are clumpsy; when two maser clouds having the same velocities are overlapping along the line of sight, their brightness temperature is greatly enhanced through "self-amplification" (Deguchi & Watson 1989); this could account for the fact that only Seyfert 2s seen nearly edge-on are detected as then the probability of seeing two aligned clouds is maximized (Kartje et al. 1999).

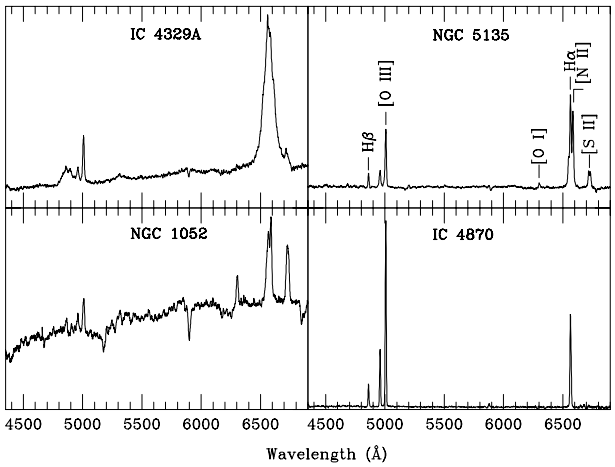

Fig. 2. Spectrum of a Seyfert 1 nucleus (IC 4329A), a Seyfert 2 nucleus (NGC 5135), a Liner (NGC 1052) and a high excitation starburst galaxy (IC 4870). These four spectra have been taken with the ESO 1.5m telescope.

H_2O masers emitted from a rotating molecular disk with a radius of the order of one parsec have been observed in two Seyfert 2s: NGC 1068 (Gallimore et al. 1996) and NGC 4258 (Greenhill et al. 1995; Miyoshi et al. 1995); both galaxies contain a massive (2-4 10^7 $M_\odot$) nuclear BH. The discovery of these molecular disks provides one of the most compelling evidence today for the existence of a massive BH in the nucleus of an AGN.

2.1.3. Diagnostic diagrams and composite nuclear spectra

Baldwin et al. (1981) have shown empirically that several combinations of easily-measured emission lines can be used to separate emission line galaxies into three categories according to the principal excitation mechanism: nuclear H II regions or starbursts, Seyfert 2s and Liners (Fig. 2 shows typical spectra of a Seyfert 1, a Seyfert 2, a Liner and a starburst galaxy). They found that the three groups can be effectively segregated using plots of [N II]λ6583/Hα *vs* [O III]λ5007/Hβ and of [O II]λ3727/[O III]λ5007 *vs* [O III]λ5007/Hβ, [N II]λ6583/Hα, or [O I]λ6300/Hα.

Veilleux & Osterbrock (1987) have proposed a revised method of classification involving the line ratios λ5007/Hβ, λ6583/Hα, [S II]$\lambda\lambda$6717,6731/Hα and λ6300/Hα. These line ratios take full advantage of the physical distinctions between the various types of objects and minimize the effects of reddening correction and calibration errors. The λ6583/Hα, $\lambda\lambda$6717,6731/Hα and λ6300/Hα ratios are well correlated with each others (Ho et al. 1997c), therefore all these diagrams should basically lead to the same classification.

The use of Veilleux & Osterbrock (1987) diagnostic diagrams generally yields an immediate classification of the nuclear emission line clouds; "transition" ob-

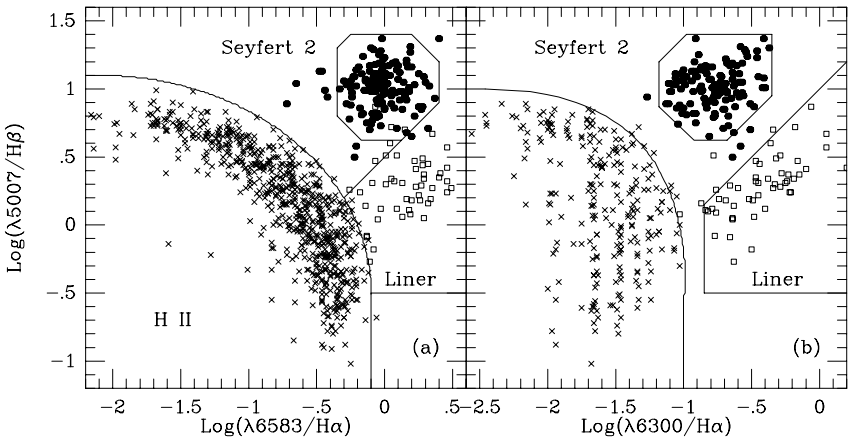

Fig. 3. Diagnostic diagrams for all nuclear emission line galaxies with published line ratios, excluding objects with a composite spectrum. The regions containing H II regions, Seyfert 2s and Liners have been drawn empirically. A few Seyfert 2s with weak [N II] lines appear outside the region assigned to Seyfert 2s. A few other objects falling in "intermediate" regions deserve a more detailed study.

jects however exist which cannot be classified unambiguously from their line ratios (Veilleux & Osterbrock 1987). When observed with sufficient spectral resolution, such objects show different profiles for the lines, this being due to the superposition of several components that have different relative strengths and are kinematically and spatially distinct, usually a H II region and a Seyfert cloud; they have a "composite" spectrum (Moran et al. 1996; Gonçalves et al. 1999).

Fig. 3 shows the Veilleux & Osterbrock diagnostic diagrams for a large number of nuclear emission line galaxies with published line ratios, excluding objects which have been shown to have a composite spectrum; we have empirically drawn lines enclosing regions containing H II regions, Liners and Seyfert 2s.

Diagnostic diagrams using near-IR lines such as [O II]$\lambda\lambda$7320,7330 and [S III]$\lambda\lambda$9069,9531 also provide a powerful method in classifying emission line galaxies (Osterbrock et al. 1992).

Several emission features in the mid-infrared (MIR) allow to distinguish between starbursts and AGNs. The 7.7μm "polycyclic aromatic hydrocarbon" (PAH) emission feature is strong in starbursts and weak in AGNs (Lutz et al. 1998; 1999). On the other hand, the high-excitation lines [O IV]λ25.9μm and [Ne V]λ14.3μm are strong relative to [Ne II]λ12.8μm in AGNs and weak in starbursts (Genzel et al. 1998; Viegas et al. 1999).

2.2. The unified model

2.2.1. The Seyfert 1.8 and 1.9 galaxies

Osterbrock (1981) defined two new subclasses of Seyferts: Seyfert 1.8s show weak, but readily visible broad Hα and Hβ emission, while Seyfert 1.9s show only broad Hα. In these objects, the broad Hα/Hβ emission line ratios are unusually large compared with those of typical Seyfert 1s, suggesting that dust may be particularly important in the BLRs (Goodrich 1990). The broad Hα/Hβ ratios for these objects range from about 5 to 15; if the intrinsic values are typical of those of Seyfert 1s, that is $\sim$ 3.1 (Baker 1997), and are modified by reddening, extinction values in the range A_V=1.2-4 mag. are implied (Goodrich 1990). A broad Paβ line has been observed in some of these objects confirming these results (Blanco et al. 1990; Rix et al. 1990).

The presence of an unresolved central continuum source in *Hubble Space Telescope* (*HST*) images is a virtually perfect indicator of a Seyfert 1 nucleus; the converse is not true; over one-third of Seyferts with direct spectroscopic evidence for broad Balmer wings show no nuclear point source; but a number of them are classified as Seyfert 1.8 or 1.9; they appear more extinguished by dust absorption than those which display a compact central nucleus (Malkan et al. 1998).

A broad Paβ line (Goodrich et al. 1994; Ruiz et al. 1994; Veilleux et al. 1997a) has been observed in a small number of Seyfert 2s, showing that they contain a heavily reddened BLR ($A_V \geq 4$ mag.) similar to that found in Seyfert 1s. A broad Paα has been found in a few NLRGs suggesting that the visual extinction in the broad line region in these objects is in the range A_V=1.5-4.5 mag. (Hill et al. 1996). AGNs with narrow optical emission lines and broad IR hydrogen lines are here called S1is.

A hidden BLR has been found by spectropolarimetry of the nucleus of a number of Seyfert 2s; the broad line emission lines are scattered into our line of sight by free electrons. But hidden BLRs are observed only in galaxies with warmer far infrared colours, indicating that the scattering particles must lie very close to the plane of the torus and therefore that, to see these lines, we must have a direct view of the inner wall of the torus (Heisler et al. 1997). The objects in which broad Balmer lines are detected by spectropolarimetry are called S1hs.

Seyfert 1 nuclei have been found to reside in earlier type galaxies than Seyfert 2 nuclei; this could be explained if the absorption in a fraction of all Seyfert 2 nuclei were due to galactic dust rather than to a dusty torus surrounding the nucleus, the galactic dust having a higher covering fraction than the torus; and indeed the Seyfert 2s are significantly more likely to show nuclear dust absorption in the form of irregular lanes and patches (Malkan et al. 1998). Oliva et al. (1999) have found that old and powerful starbursts are relatively common in Seyfert 2s while absent in genuine Seyfert 1s; this would be naturally explained if a fraction of all Seyfert 2 nuclei, located in spiral galaxies were indeed obscured by galactic dust. These objects should not show hidden polarized broad line regions.

The optical spectrum of the radio galaxy 3C 234.0 shows broad components to the Hα and Hβ lines with a Balmer decrement Hα/Hβ=7.3, implying an extinction A_V=2.2 mag.; this object could then be classified as a Seyfert 1.8, *i.e.* a Seyfert 1 whose nucleus is seen directly, although through a relatively large extinction. However, spectropolarimetry reveals strongly polarized (∼20-25%) broad Balmer lines due to scattering of the nuclear lines; the broad-line photons seen in total flux are also light scattered from the hidden nucleus; 3C 234.0 should be considered as a Seyfert 2 galaxy as no broad emission lines are seen directly from the nucleus (Tran et al. 1995; Young et al. 1998). IRAS 11058−1131 and IRAS 23060+0505 (Young et al. 1996a,b) are similar examples.

2.2.2. The X-ray properties of Seyfert 1 galaxies

The X-ray spectra of Seyfert 1s are dominated in the 2-10 keV (HX) range by a power-law component with a photon spectral index Γ=1.95 ± 0.05 (George et al. 1998a). In most Seyfert 1s, a flattening of the spectrum is observed above 10 keV (Nandra & Pounds 1994). It is satisfactorily explained by Compton reflection from cold (T<10^6K), optically thick matter (Magdziarz & Zdziarski 1995), presumably an accretion disk (Lightman & White 1988; Matt et al. 1991).

Seyfert 1s and QSOs generally do not contain significant column densities of neutral gas in excess of the Galactic value ($N_H < 10^{20}$ cm^{-2}) (Gondhalekar et al. 1997; Laor et al. 1997a) (interstellar photoelectric absorption cross sections in the range 0.03-10 keV, computed assuming solar abundances, have been published by Morrison & McCammon 1983). However Mark 6, a Seyfert 1.5, has an X-ray spectrum with complex absorption implying column densities of neutral hydrogen of ∼(3-20) 10^{22} cm^{-2} typical of a Seyfert 2 (Feldmeier et al. 1999).

In most broad emission line objects, the Fe Kα line at 6.4 keV is observed with a mean EW of 100-150 keV (Nandra & Pounds 1994). Very often, the iron line is resolved with FWHM up to ∼ 50 000 km s^{-1}; it is redshifted, asymmetric and variable. It is thought to arise from fluorescence from the innermost regions of a X-ray illuminated relativistic accretion disk close to the central BH (Sulentic et al. 1998; Nandra et al. 1999; Guainazzi et al. 1999; Iwasawa et al. 1999; Wang et al. 1999a). In other objects, such as BLRGs, the line is narrow and not variable and may be formed in the molecular torus if its hydrogen column density is larger than $N_H = 10^{23}$ cm^{-2} (Wozniak et al. 1998).

Most Seyfert 1s show evidence for an excess of soft X-rays above the hard X-ray power-law extrapolation, dominant below ∼1 keV (Turner & Pounds 1989; Walter & Fink 1993). The nature of this soft X-ray excess is still an open issue. A multi-temperature black body (with temperatures in the range 40-140 eV) gives a satisfactory fit for most of the sources (Comastri et al. 1992; Piro et al. 1997). Objects with a large UV (around λ1375Å) excess do also show a strong soft X-ray excess suggesting that the big blue bump in Seyfert 1s is an UV to soft X-ray bump; the relative strength of the big blue bump to the HX component varies by a factor of up to one hundred from object to object (Walter & Fink 1993; Walter et al. 1994).

X-ray variability is very common among Seyfert 1s; in many of these objects, the variability amplitude below 2 keV is greater than that in the hard X-ray band (Nandra et al. 1997a).

2.2.3. The X-ray properties of Seyfert 2 galaxies

The "unified model" for AGNs assumes Seyfert 2s and Seyfert 1s to be identical physical objects, while the orientation of the line of sight with respect to an obscuring torus accounts for all the observed differences between the two classes.

In agreement with this model, the X-ray emission of many Seyfert 2s is characterized by a power-law spectrum similar to that observed in Seyfert 1s, with a cut-off at low energies due to absorption by gas column densities between 10^{22} and $> 10^{24}$ cm^{-2} (Malizia et al. 1997; Sambruna et al. 1999). Such high absorbing column densities have been identified with the torus. In addition to this hard component, there is a soft component due to reflection from an optically thick disk or a molecular torus (Smith & Done 1996).

In low X-ray luminosity Seyfert 2s, in addition to the compact X-ray source associated with the nucleus, an extended X-ray component due to starburst activity can also be present (Turner et al. 1997a; Singh 1999).

For $N_H < 10^{24}$ cm^{-2}, X-rays above a few keV can penetrate the torus, making the nuclear source visible to the observer; for values of N_H around 10^{24} cm^{-2}, only X-rays in the 10-100 keV range pass through the torus. These sources are called "Compton thin"; their column density is measurable. For values of N_H higher than 10^{24} cm^{-2}, the matter is optically thick to Compton scattering and the nucleus becomes practically invisible also in hard X-rays; it can be observed only in scattered light; such sources are called "Compton thick" (Matt 1997; Bassani et al. 1999).

A number of Seyfert 2s have been found with column densities in the range 1-5 10^{24} cm^{-2}: NGC 4945 (Iwasawa et al. 1993; Done et al. 1996), NGC 6240 (Vignati et al. 1999), Mark 3 (Cappi et al. 1999), while others are Compton-thick (Turner et al. 1997b; Bassani et al. 1999). About 3/4 of all Seyfert 2s are heavily obscured ($N_H > 10^{23}$ cm^{-2}) and almost half are Compton-thick (Risaliti et al. 1999).

When the column density increases to a few 10^{23} cm^{-2}, the Fe Kα EW increases since it is measured against a depressed continuum; the EW can be higher than 1 keV for column densities $N_H > 10^{24}$ cm^{-2} (Bassani et al. 1999).

Strong observational evidences suggest that the [O III] luminosity is one of the best independent measures of the intrinsic luminosity of the nuclei of AGNs. Indeed, Seyfert 1s and 2s have the same ratio of far-infrared (FIR) to [O III] luminosities which is consistent with the hypothesis that the [O III] and FIR emissions are isotropic in both types of objects (Bonatto & Pastoriza 1997); the narrow-line luminosities of NLRGs and radio loud QSOs having the same extended radio luminosities are similar (Simpson 1998); moreover a strong correlation has been found between [O III] and HX luminosities for objects with

low N_H (Ueno et al. 1998; Xu et al. 1999). The λ5007 emission line luminosity can therefore be used to roughly infer the intrinsic power in AGNs, even in Compton-thick Seyfert 2s. It seems however that the strength of the [O III] lines is somewhat aspect-dependent, core-dominated QSOs having stronger lines than lobe-dominated QSOs (Baker 1997). If the observed X-ray luminosity is substantially less than that predicted by [O III], this is an indication of the presence of a hidden X-ray continuum source (Ueno et al. 1998; Maiolino et al. 1998; Bassani et al. 1999). As a few per cent of the soft X-rays are expected to be scattered into our line of sight, Seyfert 2s should be underluminous in the soft X-ray band by a factor of 10-100 relative to Seyfert 1s having the same [O III] luminosity (Mulchaey et al. 1992; Halpern et al. 1995).

NGC 3147 and NGC 7590 are bona-fide Seyfert 2s and yet have negligible X-ray absorption; the low absorption could be reconciled with their Seyfert 2 nature only if they were Compton-thick which is not supported by their large soft X-ray (0.1-2.5 keV) to λ5007 flux ratio (Bassani et al. 1999); these authors concluded that there might be a few objects in which the Seyfert 2 appearance is intrinsic and not due to obscuration; but what would then be the mechanism of ionization of the Seyfert 2 nebulosities which are generally believed to be photoionized by the hidden QSO?

We have collected all known AGNs with $N_H > 7\,10^{21}$ cm^{-2}, from Bassani et al. (1999), excluding NGC 1365 for which the nuclear source has a low column density (Komossa & Schulz 1998). From the most recent available data, four of these objects are now classified as Seyfert 1.9s (NGC 526a, NGC 2992, NGC 7314 and F 49; two more NGC 5674 and ESO 103−G35 could also be S1.9, but their published spectra are of poor quality; moreover in ESO 103−G35 the X-ray column density is suspected to be variable; Malizia et al. 1997), four more are S1is (NGC 2110, NGC 5506, ESO 434−G40 and IRAS 20460+1925). Thirty six objects are Seyfert 2s or S1hs (and one possible Seyfert 2); NGC 7582 is discussed below. All the Seyfert 1.9s and S1is have moderate column densities (7-37) 10^{21} cm^{-2}, while the pure Seyfert 2s have very large column densities ($>$ 40 10^{21} cm^{-2}). The ranges of column densities of the S1hs and the S2s are about the same.

RX J1343.4+0001 is a type 1.9 QSO at z=2.35; the X-ray column density is $\sim 10^{23}$ cm^{-2} which is large for a type 1.9 QSO; the nature of the UV continuum in this object is also puzzling (Georgantopoulos et al. 1999).

In table 1 we give the range of visible extinction found for the Seyfert 1.8s and 1.9s, the S1is and the pure Seyfert 2s, including the S1hs (col. 2), the column densities inferred from the X-ray observations (col. 3) and the visible extinction calculated from A_V=0.5 $N_H\,10^{-21}$ cm^{-2} (Predehl & Schmitt 1995) (col. 4). There is a clear correlation between the optical and X-ray derived values of the extinction; it seems however that the extinctions deduced from the X-ray column densities are consistently larger by about a factor of two than the extinctions obtained from the optical or infrared emission lines, in agreement with Mushotzky (1982). To explain this finding, Granato et al. (1997) suggested the existence of dust-free X-ray absorbing gas, lying inside the dust sublimation radius.

Table 1. Average extinctions and column densities

Type	A_V	N_H 10^{21} cm^{-2}	$A_V(X)$
S1.8-S1.9	1.2– 4	7–15	4– 8
S1i	4–11	16–37	8–18
S2	> 11	> 40	> 20

In conclusion, it seems that the hard X-ray properties of Seyfert 2s depend on a single parameter, the absorbing column density along the line of sight, in accordance with the unified model (Bassani et al. 1999). All Seyferts, from S1.0 to S1.9 to S2, could be quantified by their X-ray column density.

A few hard X-ray sources turned out to be associated with galaxies with strong emission lines undistinguishable from those of Seyfert 2s (Ward et al. 1978; Schnopper et al. 1978). These objects were called Narrow emission Line X-ray Galaxies (NLXGs), or more often NELGs; they more closely ressemble Seyfert 1s than Seyfert 2s at high energies, having HX luminosities in the range 10^{42}-10^{44} erg s^{-1}; they were thought to represent a new class of X-ray galaxies (Ward et al. 1978; Morris & Ward 1985; Warwick et al. 1989).

Most of them turned out to have relatively large X-ray absorbing column densities (of the order of a few times 10^{22} cm^{-2}), implying a visual absorption $A_V \sim 10$ mag. for the central engine and the broad emission line region (Warwick et al. 1993). Several of these objects were indeed found to have a weak broad Hα or Paβ component showing that they are Seyfert 1s with heavily reddened broad lines (Véron et al. 1980; Shuder 1980; Goodrich et al. 1994).

Although today the X-ray NELGs fit nicely into the Seyfert classification, being considered as either Seyfert 1.8s, 1.9s, or 2s with a relatively small column density, they are still sometimes considered as constituting a special class of objects.

The X-ray column densities observed in AGNs are usually variable, with time-scales of the order of one year or less (Malizia et al. 1997). On the other hand, some Seyferts have spectra changing from Seyfert 1.9 to 1.0 (Mark 530, Mark 993, Mark 1018); the changes in flux of the broad lines and continuum near Hα and Hβ are consistent with changes in the extinction in each of these cases (Goodrich 1989a; 1995; Tran et al. 1992). Broad Balmer lines have appeared in the nucleus of the Seyfert 2 galaxy NGC 7582 (Aretxaga et al. 1999); the X-ray column density, although not measured at the time where the broad lines were visible, was found to vary in the range 0.9-4.8 10^{23} cm^{-2} (Warwick et al. 1993; Xue et al. 1998); the apparition of the broad lines could be explained by a drop of the column density to $\sim 10^{22}$ cm^{-2} or by holes appearing in the obscuring screen (Turner et al. 1999b). It seems likely that the observed changes of optical types are due to changes of the column densities. The shortest observed time scales for spectral changes imply high transverse velocities for the dusty clouds, high enough that they must be close (but outside of) the bulk of the BLR itself (Goodrich 1995). The variability of both the X-ray column densities and the visible extinctions implies some dispersion in the correlation between these two quantities if they are not measured simultaneously, which is generally the case.

2.3. BALQSOs and warm absorbers

More than half of the Seyfert 1s show K-shell edges of warm oxygen (O VII and O VIII at 0.739 and 0.870 keV respectively), characteristic of optically thin, photoionized material along the line of sight to the central engine, the so-called "warm absorbers" (Reynolds 1997; George et al. 1998a). The column densities of the ionized material are typically in the range $N_H \sim 10^{21}$-10^{23} cm^{-2} (George et al. 1998a); in many objects, the column density is variable, but the O VII and O VIII features do not vary simultaneously leading to a two zone model (George et al. 1998b).

Warm absorber objects are generally more likely to have high optical polarization than objects with no detected ionized absorption (Leighly et al. 1997); objects displaying deep O VII edges often show significant optical reddening (Reynolds 1997; Reynolds et al. 1997; Grupe et al. 1998). These observations suggest that the warm absorber is associated with dust.

As much as 50% of all Seyfert 1s show narrow (100-300 km s^{-1}), high ionization UV absorption lines (C IV, N V, O VI, Si IV), blueshifted from 0 to 1 500 km s^{-1} and variable on time scales of weeks to years (Crenshaw 1997). The X-ray warm absorbers seem to be associated with these absorption lines (Mathur et al. 1998; Wang et al. 1999b). The iron coronal lines observed in some Seyfert 1s could be emitted by the warm absorbers (Reynolds et al. 1997).

A low-energy X-ray cut-off is sometimes found in radio loud QSOs; it is due to photoelectric absorption with column densities of $\sim 10^{21}$ cm^{-2}; these objects usually show a narrow C IV absorption line (Elvis et al. 1998).

In Seyfert 1s and QSOs, the broad Hα and Hβ luminosities are tightly correlated with (in fact proportional to) the X-ray luminosity (Koratkar et al. 1995; Yuan et al. 1998; Imanishi & Ueno 1999). However, a distinct class of "X-ray-weak" QSOs has been identified, which form $\sim$10% of the population, and where the X-ray emission is smaller by a factor 10-30 than expected from their broad Hβ luminosity (Laor et al. 1997a; Imanishi & Ueno 1999); there is a strong correlation between the soft X-ray weakness and the C IVλ1550 absorption EW which suggests that absorption is the primary cause of the soft X-ray weakness (Brandt et al. 1999b).

BALQSOs (Broad Absorption Line QSOs) are a special class of QSOs that show mostly highly ionized gas flowing away from the central source at speeds up to 10 000 to 30 000 km s^{-1} or more. The BALs appear in the spectra of about 10% of all QSOs (Turnshek 1995). The observed radial terminal velocity of the gas being ejected from BALQSOs is strongly anticorrelated with the radio power (Weymann 1997). The continuum and emission line properties of BALQSOs and non-BALQSOs are remarkably similar (Weymann et al. 1991).

BALQSOs show systematically higher optical polarization than other QSOs, the degree of polarization increasing toward shorter wavelengths; it seems that broad absorption is observed in BALQSOs because they are inclined at intermediate inclinations where our line of sight passes through gas clouds located near the surface of the dusty torus, the polarization being due to scattering by this material (Schmidt & Hines 1999; Ogle et al. 1999).

BALQSOs are very weak X-ray sources, often being 30-100 times less luminous in X-rays than expected from their optical luminosities indicating that the X-ray flux is reduced by high column densities ($N_H > 5\ 10^{23}$ cm^{-2}) of either cold or ionized material; the absence of selective reddening in BALs, combined with the high inferred X-ray column densities argues for very little dust (Gallagher et al. 1999).

In conclusion, it seems that there is a continuum of absorption properties connecting unabsorbed QSOs, X-ray warm absorber QSOs, soft X-ray weak QSOs and BALQSOs (Brandt et al. 1999b).

2.4. Fe II emission and narrow line Seyfert 1 galaxies

2.4.1. Fe II emission

Nearly all broad line AGNs have optical Fe II emission in their spectrum (Osterbrock 1977). The blend of Fe II lines between Hγ and Hβ consists of lines in multiplets 26,37,38,43 and 44 (Grandi 1981). The Fe II strength is usually measured by the quantity R4570=Fe II λ4570/Hβ, *i.e.* the relative flux in the λ4570 blend measured between λ4434 and λ4684 (see for instance Boroson & Green 1992) and in Hβ. Typical AGNs have R4570 $\sim$ 0.4 with 90% of objects in the range 0.1 to 1 (Osterbrock 1977; Bergeron & Kunth 1984). Moderately strong Fe II emission (R4570 $>$ 1) occurs in perhaps 5% of objects, but superstrong Fe II emission (R4570 $>$ 2) is roughly an order of magnitude rarer (Lawrence et al. 1988). The known superstrong Fe II emitters (Lipari et al. 1993; Lipari 1994) are listed in table 2; most are luminous/ultraluminous IR AGNs (Lipari et al. 1993).

The Fe II lines have the same widths as the broad Hβ lines, suggesting that they arise in the same region (Boroson & Green 1992). Fe II is the single largest contributor to the emission line spectrum (Wills et al. 1985). The Fe II emission in most AGNs is probably too strong to be explained by photoionization; the Fe II lines could be collisionally excited in low temperature (6 000 $<$ T $<$ 8 000 K), high density (Ne $> 10^{11}$ cm^{-3}) clouds (Joly 1987; Collin-Souffrin et al. 1988; Kwan et al. 1995; Verner et al. 1999).

Table 2. Known superstrong Fe II emitters

Name	Position	R4570	$H\beta_{br}$ FWHM km s^{-1}
PHL 1092	0137+06	6.2	1300
IRAS 07598+6508	0759+65	2.6	3200
Mark 231	1254+57	2.1	3000
Mark 507	1748+68	2.9	965
IRAS 18508−7815	1850−78	2.4	3100

Fe II is strong in objects with weak [O III] emission and vice versa (Boroson & Green 1992; McIntosch et al. 1999). The dominant source of variation in the observed properties of broad line AGNs is a physical parameter which

balances Fe II excitation against the illumination of the narrow line region; the anti-correlation could be due to an increase of the covering factor of the BLR as one moves from the strong [O III], weak Fe II objects to the weak [O III], strong Fe II objects; this sort of behaviour is thought to be dependent on the ratio of the actual accretion rate to the "Eddington accretion rate" (Boroson & Green 1992); indeed, when $\dot{M} \gg \dot{M}_{\rm Edd}$, the disk becomes geometrically thick as radiation pressure becomes competitive with gravity (Begelman 1985).

While, for Seyfert 1s and radio quiet QSOs, the Fe II EW distribution extends from $\sim$ 10 to 120Å, the steep spectrum radio sources almost all lie below 20Å. BLRGs and steep spectrum QSOs have weaker optical Fe II and stronger [O III] than either flat spectrum or radio quiet objects (Grandi & Osterbrock 1978; Joly 1991; Boroson & Green 1992).

There is a strong anticorrelation between R4570 and the FWHM of the broad Hβ component (Zheng & Keel 1991; Wang et al. 1996; Lawrence et al. 1997). In fact, the Fe II strength and line width seem to be most closely connected with continuum shape in general; strong Fe II emitters have steeper optical spectra, are more X-ray quiet, have steeper X-ray spectra and weaker blue bumps, weaker [O III], and absorption features from outflowing ionized material (Lawrence et al. 1997).

Six out of 18 QSOs with weak [O III] and strong Fe II emissions were found to exhibit a C IV BAL (broad absorption line) region which is significantly larger than the overall fraction of QSOs observed to have BAL; this suggests a covering factor of $\simeq$0.33 for the BAL region (Turnshek et al. 1997).

The relatively rare BALQSOs which show strong Mg II absorption show especially strong Fe II emission and weak [O III] lines; they are also much redder in the interval $\sim$ 1 550-2 200Å than the other QSOs (Weymann et al. 1991).

All AGNs have strong UV Fe II lines (the Fe II bump at 2 500Å), regardless of the strength of the optical Fe II lines; the intensity ratio of UV to optical Fe II emission ranges from 4 to 12 (Wills et al. 1985; Corbin 1992). The main factor determining the relative strength in the two wavelength bands are the Fe II line optical depths and the Balmer opacity; when the optical thickness increases, the intensity of the optical lines relative to the UV lines increases; a ratio of the order of 1 in the relative intensities of the optical to UV lines implies a column density of about 10^{23} to 10^{24} cm^{-2} (Joly 1981; Wills et al. 1985).

2.4.2. Narrow line Seyfert 1 galaxies

Osterbrock & Pogge (1985) have identified a class of AGNs having all the properties of the Seyfert 1s with, however, very narrow Balmer lines and strong optical Fe II lines; they are called "narrow-line Seyfert 1s" or NLS1s. Quantitatively, a Seyfert 1 is called a NLS1 if the FWHM of the "broad" component of the Balmer lines is smaller than 2 000 km s^{-1} (Osterbrock 1987) and if the ratio of [O III]λ 5007 to Hβ is < 3 (Goodrich 1989b). However, there is a continuous distribution of optical line widths in Seyfert 1s and the separation between BLS1s (broad line Seyfert 1s) and NLS1s is arbitrary (Turner et al. 1999a).

Grupe et al. (1999a) have found a few objects with "narrow" broad Balmer lines which have both weak Fe II and strong [O III], as well as objects with "broad" lines and strong Fe II and weak [O III]. Three of the superstrong Fe II emitters have relatively broad Balmer components (FWHM $> 3\,000$ km s^{-1}, see table 2).

NLS1s are generally found to be radio quiet; there are only two radio loud NLS1s known so far (PKS 0558−504 and RGB J0044+193) (Siebert et al. 1999).

The soft photon spectral index Γ (0.1-2.4 keV) of Seyfert 1s, which measures the relative strength of their soft component, is well correlated with the Balmer line width; strong soft X-ray excess objects are NLS1s (Puchnarewicz et al. 1992; Laor et al. 1994; Boller et al. 1996; Wang et al. 1996). However, Grupe et al. (1999a) have shown that this correlation holds for the high luminosity AGNs but does not appear for the low-luminosity objects.

There is a correlation between the strength of the high-ionization lines and the X-ray spectral index; strong high-ionization lines occur predominantly in objects with a soft X-ray excess (Erkens et al. 1997). In NLS1s, [Fe VII] λ6087 and [Fe X]λ6375 are often present in emission (Goodrich 1989b).

The soft excess component of NLS1s can be modelled by a black body with temperatures in the range 0.1 to 0.25 keV (Leighly 1999b; Vaughan et al. 1999a), rather similar to the temperature range found for the BLS1 soft excesses. It is often so strong that it rules out models in which the soft excess is produced through reprocessing of the hard continuum (Vaughan et al. 1999a).

NLS1s very frequently exhibit rapid and/or high-amplitude X-ray variability (Boller et al. 1996; Forster & Halpern 1996; Molthagen et al. 1998; Vaughan et al. 1999b). They have larger amplitudes than the BLS1s (Fiore et al. 1998). The nuclear component of NGC 4051 shows strong soft X-ray variability with X-ray intensity changing by a factor 2-3 on a time-scale of a few 100 sec (Singh 1999); it has also been observed once while its HX flux was about 20 times fainter than its historical average value; the observed flat spectrum and intense iron line (EW $\sim$ 600 eV) are best explained assuming that the active nucleus has switched off, leaving only a residual reflection component visible (Guainazzi et al. 1998). Observed variabilities by a factor $\sim$2 in a few hours show that a substantial fraction of the soft component comes from a compact region, smaller than a light-day; this radiation must therefore be seen directly and not be reprocessed by a larger region (Turner & Pounds 1988; Boller et al. 1996). Giant-amplitude X-ray variability (up to about two orders of magnitude) has been observed in IRAS 13224−3809 (Boller et al. 1993; 1997), PHL 1092 (Forster & Halpern 1996; Brandt et al. 1999a), RE J1237+264 (Brandt et al. 1995; Grupe et al. 1995a), W 7 (Grupe et al. 1995b) and RX J0947.0+4721 (Molthagen et al. 1998).

There is a very strong anticorrelation between the Hβ FWHM and the amplitude of X-ray variability in the $\sim$0.5-10 keV bandpass; this correlation is consistent with rapid variability and narrow lines being a result of a small cen-

tral mass (Leighly 1999a; Turner et al. 1999a).

Standard accretion disks are not able to account for the soft X-ray excess unless the Eddington ratio is close to unity (Collin-Souffrin 1994; Pounds et al. 1995). The observed correlation between short-term X-ray variability and spectral steepness leads to the same conclusion (Fiore et al. 1998; Brandt 1999).

If the broad-line emitting region is gravitationally linked to the central BH, one can show that the FWHM of the lines depends on the mass of the BH, the ratio of the luminosity to the Eddington luminosity and the angle between the rotation axis of the gas disk and the line of sight. The NLS1s could be objects with a low mass BH radiating near the Eddington limit, while the AGNs with relatively narrow broad Balmer lines but with strong [O III] and weak Fe II could be AGNs seen perpendicularly to the disk (Wang et al. 1996; Laor et al. 1997a).

A serious concern for models based upon a fundamental difference in central mass is that Rodriguez-Pascual et al. (1997) found broad components to UV emission lines of both NLS1s and BLS1s while Bischoff & Kollatschny (1999) have observed variable broad (4 900 km s^{-1} FWHM) line components in the spectrum of the NLS1 Mark 110.

NGC 5905 (Bade et al. 1996; Komossa & Bade 1999), RX J1242.6−1119 (Komossa & Greiner 1999) and RX J1624.9+7554 (Grupe et al. 1999b) are interesting cases. All three are highly variable X-ray sources; in the high state, the spectra are extremely soft; optical spectra, taken several years after the X-ray outburst in each case, show no signs of Seyfert-like activity. Komossa & Bade (1999) suggested that these high amplitude X-ray outbursts could be explained by tidal disruption of a star by a central supermassive BH.

2.5. Ultraluminous infrared galaxies

The Infrared Astronomical Satellite (IRAS) surveyed $\sim$ 96% of the sky in four infrared wavelength bands centered at 12, 25, 60 and 100 μm and detected about 250 000 point sources; several thousands of them have been identified with galaxies; the majority of IRAS galaxies are starbursts, so much so that "IRAS galaxy" is sometimes used instead of starburst galaxy; however, some of them are AGNs (Soifer et al. 1987).

One of the most exciting results of the IRAS survey was the discovery of galaxies of quasar-like luminosity emitting almost entirely in the infrared; they have been called ultraluminous infrared galaxies (ULIGs) and are defined as having $L_{FIR} > 10^{12}$ $L_{\odot}$, or $L_{FIR} > 3.8\,10^{45}$ erg s^{-1}.

The FIR flux density between 42.5 and 122.5 μm has been defined as: S_{FIR} (erg s^{-1} cm^{-2}) $= 1.26\,10^{-11}$ $(2.58 S_{60\mu m} + S_{100\mu m})$ where $S_{60\mu m}$ and $S_{100\mu m}$ are the IRAS flux densities (Jy) at 60 and 100 μm respectively (Helou et al. 1985).

QSOs with $M_B=-24.0$ have a luminosity, between 1 μm and 1 keV, L$\sim 10^{12.2}$ $L_\odot$, *i.e.* ULIGs have the luminosity of low luminosity QSOs.

About 30% of all ULIGs have Seyfert type optical spectra (Wu et al. 1998; Veilleux et al. 1999); but the fraction of Seyferts among ULIGs increases dramatically above $L_{FIR}=10^{12.65}$ $L_\odot$; nearly one-half of the galaxies brighter than this limit present Seyfert characteristics, while only ~20% of the weaker ULIGs and 15% of the galaxies with 10^{11} $L_\odot < L_{IR} < 10^{12}$ $L_\odot$ have such characteristics (Veilleux et al. 1999). We should however be aware that at very high FIR luminosities, a number of ULIGs are enhanced either by gravitational lensing or by relativistic beaming. We have compiled a list of 12 ULIGs with $L_{IR} > 10^{13}$ $L_\odot$; 3 are classified as starburst, 1 as a Seyfert 2 and 8 as Seyfert 1s (75% Seyferts); but two Seyfert 1s are gravitationally lensed (IRAS F10214+4724 and APM 08279+5255) and four are HPQs (PKS 0420−01, PKS 0537−441, 3C 345.0 and 3C 446); ignoring these six objects, the fraction of Seyferts drops to 50%. Gopal-Krishna & Biermann (1998) showed that the space densities of ULIGs and QSOs are quite similar at small redshifts for $L_{bol} > 10^{12.35}$ $L_\odot$.

Nearly all ULIGs appear to be advanced merger systems, including those which have a Seyfert spectrum (Borne et al. 1999; Rigopoulou et al. 1999; Surace et al. 1999).

Merger-induced shocks are likely to leave the gas from both galaxies in dense molecular form which will rapidly cool, collapse, and fragment; thus a merger might be expected to result in a burst of star formation of exceptional intensity (Joseph & Wright 1985).

Indeed, ULIGs contain large nuclear concentrations of molecular gas detected in the millimeter lines of CO. CO maps show rotating disks of molecular gas that has been driven into the centers of the mergers; the derived gas mass, of the order of 10^9-10^{10} $M_\odot$, is equal to the mass of molecular clouds in a large, gas-rich spiral galaxy (Downes & Solomon 1998).

There is evidence that starbursts are responsible for the IR emission of even the most luminous IRAS galaxies. Most ULIGs contain a compact but resolved (>0.25") radio source obeying the FIR-radio correlation followed by starbursts (Condon et al. 1991; Sopp & Alexander 1992); the FIR-mm spectra of ULIGs can be satisfactorily modelled with spherically symmetric dust clouds with high optical depths heated by a starburst (Rowan-Robinson & Efstathiou 1993; Rigopoulou et al. 1996).

There is ample observational evidence that ULIGs which do not have a Seyfert spectrum do not contain a hidden QSO.

Spectropolarimetric and near-infrared spectroscopic observations have shown that most, if not all, ULIGs with a Seyfert 2 spectrum contain a hidden QSO, while none of the ULIGs without a Seyfert spectrum shows any obvious sign of an obscured BLR, despite the fact that the extinction at 2 μm is 1/10 that at optical wavelength (Goldader et al. 1995; Veilleux et al. 1997; Tran et al. 1999; Murphy et al. 1999).

A starlike nucleus is seen in 15% of the near-infrared *HST* images of ULIGs; but these objects are those that have been classified as Seyfert 1s or 2s (Borne et al. 1999).

Mid-infrared spectroscopic observations (3-11.6 μm) of a number of ULIGs have not led to the discovery of Seyfert nuclei not previously known from optical spectroscopy although they can probe heavily reddened ($A_V \sim 50$ mag) regions; they confirmed that the fraction of Seyfert galaxies increases with ULIG luminosities (Lutz et al. 1998).

When a QSO is found in an ULIG, its luminosity is usually too low to power the ULIG; when both an AGN and a starburst occur concurrently in an ULIG, the starburst dominates the luminosity output (Rigopoulou et al. 1999). Wilman et al. (1998) have been unable to detect a soft X-ray (0.1-2.4 keV) source at the position of five ULIGs (three Seyfert 2s and two starbursts), with an upper limit $L_X/L_{bol} \sim 2.3\ 10^{-4}$. In QSOs, the mean value of L_X/L_{bol} is ~ 0.05 (Mulchaey et al. 1992); if ULIGs are powered by a hidden QSO, the observed limits imply that less than 0.005 of the X-ray QSO luminosity is scattered into our line of sight which is much smaller than the scattering fraction inferred in the optical (a few per cent). It follows that even the three observed ULIGs with a Seyfert 2 spectrum cannot contain a QSO bright enough to power the ULIG.

Near-infrared imaging of 12 ULIGs having a Seyfert spectrum (six type 1 and six type 2) reveals, in every case, an unresolved component, coincident with the optical nucleus which increasingly dominates the emission at long wavelengths. For seven of these objects only, the dereddened nuclear luminosity is sufficiently high that they could provide the bolometric luminosity (Surace & Sanders 1999).

PKS 1345+12 is an ULIG containing a Seyfert 1 nucleus; it is an interacting system containing $3.3\ 10^{10}\ M_\odot$ of molecular gas associated with the Seyfert nucleus suggesting that the molecular gas is the fuel source rather than the AGN (Evans et al. 1999).

In conclusion, it seems that those ULIGs which do not have a Seyfert 1 or 2 optical spectrum do not host a burried AGN significantly contributing to the energetics of the objects and are powered by starbursts produced by the merging of two spiral galaxies. Those ULIGs which contain an AGN are also, most probably, powered by starbursts; but it is possible that, in some of them, the AGN is bright enough to significantly participate to the powering (Soifer et al. 1999); the AGNs themselves are likely powered by the merging process (Joseph 1999; Sanders 1999).

3. LINERS

Heckman (1980) has defined Liners as galaxies which have a nuclear optical spectrum dominated by emission lines from low excitation species ($\lambda 3727 > \lambda 5007$ and $\lambda 6300 > 1/3\ \lambda 5007$). Liners occur preferentially in galaxies of early Hubble type. They are characterized by lines whose widths are similar to those in the narrow-line region of Seyferts but whose luminosity is generally low.

The excitation mechanism of Liners has been highly controversial. Excitation mechanisms that have been proposed include photoionization by a dilute power-law continuum, shock heating, cooling flows, and photoionization by very hot

Wolf-Rayet stars or normal O stars (Filippenko 1996). Liners may be due to a variety of apparently similar but physically distinct phenomena (Heckman 1987).

3.1. Liners and AGNs

The detection of weak broad Hα emission (Ho et al. 1997b; Barth et al. 1999b), a point like X-ray source (Komossa et al. 1999), a compact ultraviolet nucleus (Barth et al. 1998) and/or a compact variable radio core (Heckman 1980) in a number of Liners supports the hypothesis that some of them are low-luminosity AGNs. By analogy with the nomenclature established for Seyferts, Ho (1998) suggested to extend the "type 1" and "type 2" designation to include Liners (L1 and L2).

The overall optical to near-infrared spectral features of Liners with a compact ($r < 200$ pc) emission line region are adequately reproduced by photoionization calculations which assume a non stellar ionizing continuum, solar abundances, and ionization parameters in the range $\sim 10^{-3}$ to 10^{-4}; allowance for variations in the total hydrogen density and in the hardness of the ionizing continuum accounts for the range of observed line intensity ratios (Ho et al. 1993a, b). The existence of a strong correlation between line width and critical density for de-excitation in the narrow-line region of some well studied Liners shows that the range of densities within each of these regions is indeed very large (N_e=10^3-10^7 cm^{-3}) (Filippenko & Halpern 1984; Filippenko 1985). The weakness of He II emission in Liners is a well known problem and indicates that the continuum illuminating the NLR clouds must contain few photons more energetic than 54 eV, the ionization potential of He^+; this problem has not yet been convincingly solved (Binette et al. 1996; Barth et al. 1996; 1997).

The S0 galaxy NGC 7213 has broad Balmer lines and is therefore certainly an AGN; its narrow-line spectrum is that of a Liner; the nuclear IR to UV continuum is similar to that of a typical Seyfert 1 (Halpern & Filippenko 1984). NGC 5252 contains a nuclear emission component which has a Liner spectrum in addition to extranuclear knots having Seyfert 2 spectra (Gonçalves et al. 1998). In both cases, photoionization by a non stellar continuum is the most likely mechanism of excitation, the low-ionization lines indicating that the ionization parameter is lower than in classical Seyferts.

However, Gonçalves et al. (1999) have shown that the distribution of the λ6300/λ5007 ratios for Seyfert 2s and Liners is probably bimodal. If Liners were similar to Seyfert 2s, the only difference being a smaller value of the ionization parameter, we would probably expect a continuous distribution of the values of this ratio. We shall see below (sec. 4.5.2) that most Liners may differ drastically from Seyfert 2s by the presence in their center of a geometrically thick rather than thin disk.

3.2. Liners and cooling flows

Clusters of galaxies are luminous X-ray sources. The bulk of the X-ray emission arises from Bremsstrahlung and line radiation processes in a hot ($T \sim 10^7$ K)

intracluster medium. In the most luminous systems, the 2-10 keV luminosity exceeds 10^{45} erg s^{-1} and the emission extends to radii $>$ 2 Mpc. The total mass of the intracluster medium exceeds that of the galaxies by factors 1-5. In the outer regions of clusters (r $>$ 1 Mpc), the intracluster medium is highly diffuse (Ne $\sim$ 10^{-4} cm^{-3}) and the cooling time far exceeds the Hubble time ($t_{cool} > 10^{11}$ yr). In the central regions of most clusters, however, the density of the intracluster medium rises sharply and the cooling time is significantly less than the Hubble time ($t_{cool} < 10^{9}$ yr). In the absence of forces other than the thermal pressure and gravity, the cooling of the intracluster medium will lead to a slow net inflow of material towards the cluster center, a process known as "cooling flow" (Allen & Fabian 1997). 40% of the clusters from an X-ray flux-limited sample have flows depositing more than 100 $M_\odot$ yr^{-1} throughout the cooling region (Peres et al. 1998). Large masses of X-ray absorbing material are common in cooling flows (Allen et al. 1999); the mass of the absorbing material is typically $\sim$ 10% of the mass of the X-ray emitting gas in the same region. Theoretical studies of the physical conditions in cooling flows suggest that the X-ray absorbing gas is likely to take the form of small, cold, mainly molecular clouds. Most of the mass deposited by the cooling flows in the central regions of the clusters must reside in some form other than X-ray absorbing gas, perhaps low-mass stars or brown dwarfs (Allen & Fabian 1997).

Molecular hydrogen has been detected from three central cluster radio galaxies in cooling flows (Jaffe & Bremer 1997). CO has been detected in the center of the Perseus cluster indicating a total molecular hydrogen mass of $\sim$ $6\,10^{10}$ $M_\odot$ (Bridges & Irwin 1998).

The central region of cooling flow clusters often (35%) show optical-line nebulosity which can be extended (up to 20 kpc) and luminous (above 10^{43} erg s^{-1} in Hα in a few cases). The emission line spectra are characteristic of Liners (Voit & Donahue 1997; Crawford et al. 1999). The emission line luminosity is correlated with the X-ray luminosity of the clusters (Donahue et al. 1992; Allen et al. 1992).

Central cluster galaxies with emission lines exhibit strong UV/blue continua in comparison to normal giant elliptical galaxies (gEs); the excess blue continuum has a similar spatial extent ($\sim$5-10 kpc) as the emission line nebulosities. These continua are better described as due to young stars than by power-law emission models; the use of simple stellar population models shows more than 10^6 O stars to be present in the most luminous systems; large B, A and F star populations are also inferred. The observed Hα flux is found to be roughly equal to the predicted flux due to O stars (Allen 1995; Smith et al. 1997; Sarazin & McNamara 1997). Filippenko & Terlevich (1992) and Shields (1992) have shown that hot, yet normal main sequence O stars (O5 or earlier) irradiating relatively dense clouds of gas can produce line ratios very similar to those observed in the central galaxy of cooling flow clusters.

Large cooling flows tend to have luminous galaxies and powerful radio sources at their center (Peres et al. 1998). Radio sources associated with central galaxies of cooling core clusters are either FR Is or amorphous (Ball et al. 1993). Burns (1990) has found that 71% of the cD galaxies with X-ray cooling core are radio loud, whereas a smaller but still significant 23% of cDs without cooling

core were detected. This disparity is striking and must point to an intimate connection between the processes giving rise to the radio and the X-ray emissions. A possible explanation is that some of the cooling gas reaches the central engines and powers the radio emission (Ball et al. 1993). Among the radio galaxies in non cooling core clusters, there are luminous and extended wide angle tails, demonstrating that mechanisms other than gas inflow from the cluster can generate relatively powerful extended radio sources in clusters (Gomez et al. 1997). Optical nebulosity is common in those cooling flows with a central radio source, but no correlation is found between optical and radio luminosities in objects with both (Fabian 1994).

Liners in FR I radio galaxies are generally supposed to be AGNs, while those found in cooling flow clusters are generally extended and probably excited either by shocks or by young stars formed by the cooling flow. But what is then the excitation mechanism of Liners found in FR I radio galaxies which are the central galaxy of cooling flow clusters?

3.3. Liners and ULIGs

About 40% of all ULIGs have Liner type optical spectra (Wu et al. 1998; Veilleux et al. 1999). Spectropolarimetric, near-infrared spectroscopic and MIR spectroscopic observations have been carried out in a number of such objects; none of them shows any obvious sign of an obscured BLR, suggesting that they are powered by starbursts (Veilleux et al. 1997; Tran et al. 1999; Lutz et al. 1999; Taniguchi et al. 1999).

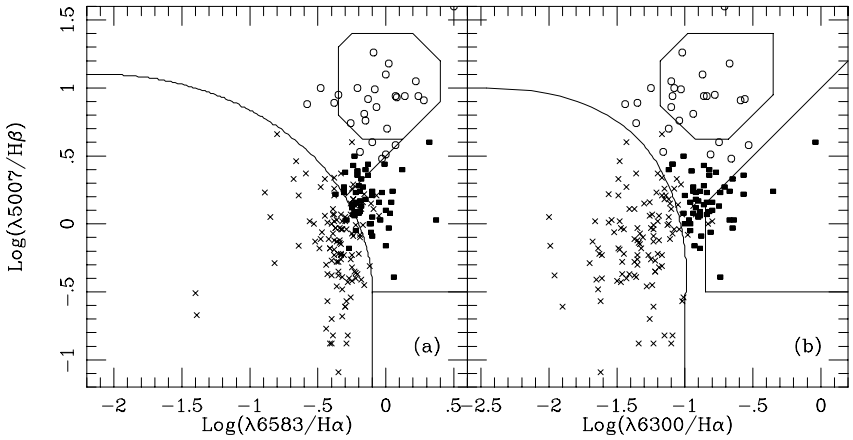

Fig. 4. Diagnostic diagrams for luminous and ultraluminous IR galaxies, excluding Seyfert 1s. The regions containing H II regions, Seyfert 2s, and classical Liners have been delineated as in fig. 3. H II regions are shown as crosses, Seyfert 2 as open circles. The black squares are the objects called "Liners" in the original papers (see text); they cluster in a region which is well outside the region occupied by the "classical" Liners, *i.e.* Liners associated with an AGN.

We have plotted on the diagnostic diagrams $\lambda5007/\mathrm{H}\beta$ *vs* $\lambda6583/\mathrm{H}\alpha$ and $\lambda6300/\mathrm{H}\alpha$ all luminous and ultraluminous IR galaxies for which the required

line ratios have been published (Wu et al. 1998; Veilleux et al. 1999), excluding the Seyfert 1s for which the relative fluxes of the narrow component of the Balmer lines are generally not available. These plots are shown in fig. 4. The two objects with the strongest [O I] lines are PKS 2338+03, a radio galaxy and NGC 6240, a well known AGN (Vignati et al. 1999). Comparison with fig. 3 shows that in addition to low excitation H II regions and Seyfert 2s, there is a cluster of objects around $\lambda 5007/H\beta \sim 1.6$,$\lambda 6583/H\alpha \sim 0.8$ and $\lambda 6300/H\alpha \sim 0.1$; these are the objects which have been classified as Liners; however they seem to be different from the Liners in fig. 3 which are mostly associated with AGNs, suggesting that, indeed, they are not genuine AGNs.

3.4. Emission lines in giant elliptical galaxies

In more than half of the optically selected nearby gE galaxies, nuclear emission lines have been detected. The ionized gas typically has an extended distribution (1-10 kpc) and can have a plethora of different morphologies: flattened disk-like structures, filamentary structures etc. (Goudfrooij et al. 1994; Macchetto et al. 1996). Most of these objects are genuine Liners (Ho et al. 1997c) and show indication of an AGN (unresolved broad wings of Hα, strong radio or X-ray emission) (Alonso-Herrero et al. 1999). Their Hα luminosity is weak ($3\,10^{37}$ to $5\,10^{40}$ erg s^{-1}) (Goudfrooij et al. 1994; Macchetto et al. 1996).

E galaxies contain dust, cool gas (H I, T $<$ 10^2 K) and warm gas (H II, T $\sim$ 10^4 K) which could be either external to the galaxy resulting, for example, from a cooling flow or the merging of two galaxies, or internal to the galaxy through stellar mass loss. Knapp et al. (1985), Kim (1989), Forbes (1991), Bertola et al. (1992) and Goudfrooij & de Jong (1995) argued that the gas as well as the dust is of external origin in the majority of cases.

Extended X-ray emission from individual E galaxies due to hot interstellar gas has been reported; radiative cooling may (Thomas et al. 1986) or may not (Brown & Bregman 1998) be important throughout most of this gas. Fabian et al. (1986) pointed out that small X-ray cooling flows may explain the presence of Liners in ordinary galaxies. Stocke et al. (1991) have isolated a class of luminous X-ray sources ($L_X > 10^{43.5}$ erg s^{-1}) that they call "cooling flow galaxies" which are associated with E galaxies not located within a rich cluster and having an optical spectrum similar to the spectra of the dominant galaxies in cooling flow clusters.

Post-AGB stars present in E galaxies could provide sufficient ionizing radiation to account for the observed Hα luminosity in these galaxies and to reproduce the excitation level of the ionized gas (Binette et al. 1994).

In conclusion, the Liners found in E galaxies could be a mixed population containing both AGN-type Liners ionized by a non-stellar central continuum and objects in which the ionization is provided by hot stars.

Liner nuclei are found not only in E galaxies, but also in S0s and early type spirals ; many of these galaxies are transition objects with spectra appearing to be intermediate between those

of H II regions and Liners; their low ionization lines are stronger than those of the former, yet weaker than those of the latter; they have been called weak-[O I] Liners (Ho et al. 1997c).

Some of them are probably composite H II/Liner systems (Binette 1985; Ho et al. 1993a); others could be photoionized by hot ($>$ 45 000 K) main-sequence O stars (Filippenko & Terlevich 1992); however, Alonso-Herrero et al. (1999), from near-infrared spectroscopy ([Fe II]λ1.2567μm and Paγ) of a number of them, suggested that they could rather be due to ionization by aging starbursts in which the supernova remnants (SNRs) play an increasingly important role as the starburst ages and the hot stars fade while a high supernova rate persists: the Fe II line is predominantly excited by SNR-driven shocks and the Pβ tracks H II regions excited by massive young stars. The weak X-ray emission of these objects seem to be of stellar origin (Terashima et al. 1999).

25% of the observed Liners hosted in a spiral display a compact (but not always unresolved) nuclear UV source; the two observerd galaxies with an unresolved nuclear UV source have broad Hα emission (Barth et al. 1998). UV spectra show clear absorption-line signatures of massive stars in about half of them, indicating a stellar origin for the UV continuum; the stellar population in these objects could provide enough ionizing photons to explain the observed optical emission line flux thus showing that they are probably not associated with an AGN (Maoz et al. 1998).

Komossa et al. (1999) have investigated the X-ray properties of 13 S0 to Sb galaxies having a Liner spectrum; eight have been detected at rather low luminosity level; but three sources are best described by a single AGN-like power-law with X-ray luminosity above that expected from discrete stellar sources; these spectra most likely indicate the presence of low-luminosity AGNs.

Thus it appears that Liners found in spiral galaxies could be either AGNs or starbursts.

4. RADIO GALAXIES

4.1. FR I and FR II galaxies

FR Is have been defined as having low radio brightness regions further away from the galaxy than the high brightness regions (edge-darkened morphologies), while FR II have high brightness regions further away from the galaxies than the low-brightness regions, *i.e.* they are the classical double radio sources with edge-brightened lobes (Fanaroff & Riley 1974). The Fanaroff-Riley classification is somewhat subjective; although most objects can be assigned without ambiguity to one or the other classes, there are a number of intermediate objects which are difficult to classify (Blundell et al. 1999). FR Is generally have a 178 MHz luminosity below $\sim 2.5\,10^{33}$ erg s^{-1} Hz^{-1} while FR IIs are stronger than this value (Fanaroff & Riley 1974); the division in power between the two classes is however not sharp, but when radio sources are plotted as points in the radio luminosity-optical luminosity plane, the Fanaroff-Riley break becomes very sharp, with the break radio power approximately proportional to the optical luminosity squared, ranging from $3\,10^{31}$ erg s^{-1} Hz^{-1} for $M_R = -21$ to $4\,10^{33}$ erg s^{-1} Hz^{-1} for $M_R = -24$ at 1400 MHz (Ledlow & Owen 1996).

Most radio galaxies contain a jet and a flat spectrum radio core.

FR IIs jets are generally one sided (Bridle 1984). The depolarization of the lobes is systematically stronger on the counter-jet side, suggesting that the visible jet is on the near side of the source indicating that the jet asymmetry is due to the presence of relativistic beaming (Garrington & Conway 1991; Laing 1988).

The large jet-counterjet brightness ratio observed in radio loud QSOs requires characteristic jet speeds > 0.6 c on kiloparsec scales (Wardle & Aaron 1997).

At parsec-scales, FR Is also have one-sided jets implying relativistic speeds ($v/c \sim 0.9$); these jets decelerate to non relativistic speeds within ~ 2 kpc from the nucleus becoming symmetrical (Lara et al. 1997; Laing et al. 1999). At kpc-scales, they are most probably turbulent, subsonic flows with velocities of the order of 1 000-10 000 km s^{-1} (Bicknell et al. 1990; Bicknell 1994). In the FR I source 3C 264.0, the jet seems to be relativistic ($\gamma \sim 5$ where $\gamma = (1-\beta^2)^{-0.5}$ is the Lorentz factor and β=v/c) near the nucleus (< 300 pc) (Baum et al. 1997); apparent superluminal transverse motion has been measured in the FR Is M 87 (Biretta et al. 1995) and B2 1144+35 (Giovannini et al. 1999).

The kinematic Doppler factor δ of a source moving in a direction making an angle θ to the line of sight and having an intrinsic Lorentz factor γ is defined as: $\delta = [\gamma\ (1 - \beta\ cos\theta)]^{-1}$.

If S_o is the unbeamed flux of the nucleus, the observed value for the same object having its intrinsically symmetric jet making an angle θ with the line of sight would be (Wall & Jackson 1997):

$$S(\theta) = S_o\{[\gamma(1 - \beta\cos\theta)]^{-p} + [\gamma(1 + \beta\cos\theta)]^{-p}\}$$

with p=3+α or p=2+α for a single sphere or a continuous jet respectively, α being the spectral index ($S_\nu \propto \nu^{-\alpha}$) (Vermeulen & Cohen 1994). For a given value of β, the maximum value of S/S_o is obtained for θ=0°; for relativistic jets and small values of θ, $S(\theta) \sim S_o\ \delta^p$; S/S_o is minimum for θ=90°, in which case, $S/S_o = 2\ \gamma^{-p}$; the ratio of the maximum to the minimum value of S/S_o is $2\ (1-\beta)^{-p}$ which is equal to 80 000 if p=2 and γ=10. Fig. 5 shows the change of the boosting factor S/S_o with the angle θ for various values of γ.

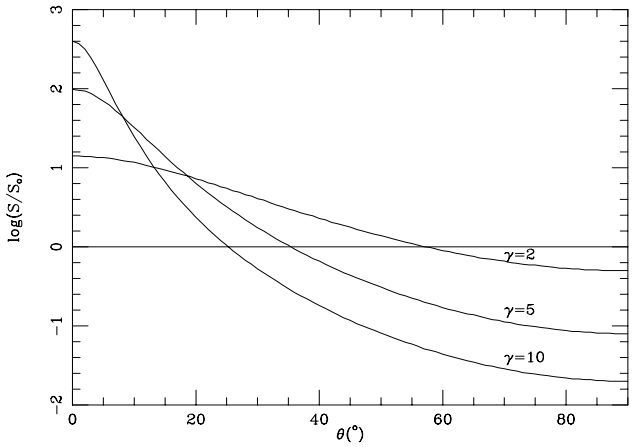

Fig. 5. Changes of the boosting factor S/S_o with the viewing angle θ, for various values of γ.

We call R the flux ratio of the core to the extended components and R_o the value of R for an unbeamed source. In FR Is and FR IIs, the core luminosity is correlated with the extended radio power, the median value of R decreasing from 10^{-1} to 10^{-3} when the extended radio power (at 1 400 MHz) increases from 10^{30} to 10^{34} erg s^{-1} Hz^{-1}; the dispersion is however large (Giovannini et al. 1994; Slee et al. 1994; Morganti et al. 1995; Zirbel & Baum 1995). Part of this dispersion is due to the fact that the jets are randomly oriented with respect to the line

of sight (Giovannini et al. 1994). The observed values of R span a wide range of values; the most lobe-dominated sources have ratios as low as R$\sim 10^{-5}$; in contrast, the most core dominated sources can have R$\sim 10^{3}$ (Jackson & Wall 1999).

As the extended emission of radio sources is unbeamed, statistically the ratio of the observed R value of any single object to the median value of R for radio objects having the same extended radio power will be a rough estimate of the enhancement factor (note however that the median value of R which is equal to R(60°) is not equal to R_o).

For NLRGs, θ is larger on average than $\sim 60°$ as objects with $\theta < 60°$ would generally appear as BLRGs or QSOs (Zirbel & Baum 1995). For this reason, QSOs and BLRGs tend to have relatively more powerful radio cores (by about a factor of ten) than NLRGs having the same extended luminosity (Fernini et al. 1997; Morganti et al. 1997; Hardcastle et al. 1998).

Monte Carlo simulations of the P_{tot} *vs* P_{core} diagram showed that the minimum Lorentz factor γ is below ~ 3.0 for FR Is sources (Morganti et al. 1995) and above $\sim$3.0 for FR IIs (Morganti et al. 1995; Hardcastle et al. 1999). Wall & Jackson (1997) chose to model the Doppler beaming of the FR I and the FR II populations with a single Lorentz factor and a single intrinsic flux ratio R_o for each parent population and took p=2; Monte Carlo simulations gave R_o=0.01 and γ=10.3 for the FR Is and R_o=0.004 and γ=20 for the FR IIs. So, although these studies give significantly different values for the Lorentz factors, they agree on the fact that they are smaller in FR Is than in FR IIs.

Spatial and spectral measurements show that both resolved (thermal) and unresolved X-ray emission in FR Is are common, although the relative strength and size of the resolved component varies between objects; the thermal extended emission comes either from hot galactic corona or from intracluster gas; the unresolved X-ray component correlates well with the core radio emission (Trussoni et al. 1997; Hardcastle & Worrall 1999). The nuclear components do not seem to show any sign of absorption (Trussoni et al. 1999).

4.2. Host galaxies of FR I and FR II radiosources

FR Is and FR IIs are associated with E galaxies (Martel et al. 1999); no FR I or FR II radio galaxies are known to have any spiral structure (Véron & Véron-Cetty 1995; see however Ledlow et al. 1999), while radio quiet Seyfert galaxies are nearly all hosted by spirals. FR I radio galaxies are optically indistinguishable from randomly selected radio-quiet cluster galaxies (Ledlow & Owen 1995). The host galaxies of FR IIs are generally gE galaxies, but not first rank cluster galaxies (Lilly & Prestage 1987; Zirbel 1996).

The host galaxy of radio QSOs (which always have an FR II morphology) have the same absolute magnitude distribution as the FR II radio galaxies, suggesting that they are also gE galaxies; the radio quiet QSO host galaxies are somewhat fainter, leading to the conclusion that spiral galaxies host Seyferts with some higher luminosity extension among the radio quiet QSOs, while E galaxies host radio QSOs and a substantial part of the radio quiet QSOs (Véron-Cetty & Woltjer 1990). *HST* images of a number of QSOs have confirmed

these findings (Bahcall et al. 1997; Boyce et al. 1998; McLure et al. 1999).

The parent galaxies of FR IIs frequently exhibit peculiar optical morphologies (tails, fans, bridges, shells and dust lanes) suggesting that they probably arise from the collision or merger of galaxy pairs, at least one member of which is a disk galaxy (Smith & Heckman 1989; Zirbel 1996). Morphological studies of QSO host galaxies by the *HST* have revealed that a sizable fraction of them show twisted, asymmetric, or disturbed isophotes or possess close small companion galaxies (Boyce et al. 1999; Lehnert et al. 1999); numerical simulations show that they are tidally formed by a gas-rich major galaxy merger (Bekki 1999).

A large fraction of FR I radio galaxies shows evidence of ongoing or past interaction or merging processes; these interactions seem not to involve gas-rich galaxies (González et al. 1993; Colina & de Juan 1995; Martel et al. 1999).

FR I clustering environments are consistent with environments about as rich as Abell richness 0; the FR II galaxies are in environments which are significantly poorer (by a factor 2-3) (González et al. 1993; Zirbel 1997). FR IIs often inhabits richer cluster environments at z$\sim$0.5, but almost totally avoid them at low redshift; FR Is show no change in environment between the two epochs (Hill & Lilly 1991).

It results from these observations that the host galaxies of FR Is and FR IIs are different implying that FR IIs cannot evolve into FR Is or vice-versa (Owen & Laing 1989; Hill & Lilly 1991). However, for Scheuer (1993), the sharp division between FR Is and FR IIs suggests that FR IIs could decay into FR Is; he noted, in support of this assumption, the evidence indicating that the more powerful FR II radio galaxies, and perhaps radio-loud QSOs too, generally live in clusters.

4.3. Emission line spectra of radio galaxies

4.3.1. FR II radio galaxies

The average emission line properties of BLRGs and radio loud QSOs on the one hand and Seyfert 1s and radio quiet QSOs on the other hand appear to be very similar (Grandi & Osterbrock 1978; Steidel & Sargent 1991; Corbin 1992). A bright unresolved point source always dominates the optical core of BLRGs (Martel et al. 1999). Differences between the optical spectra of NLRGs and Seyfert 2s are very minor (Cohen & Osterbrock 1981). Most NLRGs show prominent broad Balmer lines in polarized light (Cohen et al. 1999).

However, a number of FR IIs are known with emission lines of very low excitation or lacking emission lines completely, being spectroscopically similar to FR Is; these objects have relatively low radio luminosities; they have been called low-excitation radio galaxies or LERGs (Laing et al. 1994; Tadhunter et al. 1998). A few of these objects have radio morphologies intermediate between the FR I and FR II classes; but most are *bona fide* FR IIs. The optical properties of LERGs are probably isotropic as no broad lines are detected although a few objects show strong radio cores and other indications of beaming; *i.e.* they should not contain a dust torus and should not show broad emission lines whatever their

angle to the line of sight (Laing et al. 1994).

Radio powers and narrow emission line luminosities are strongly correlated over five orders of magnitudes for high-excitation FR II galaxies (Jackson & Rawlings 1997; Tadhunter et al. 1998; Willott et al. 1999).

4.3.2. FR I radio galaxies

FR Is generally have Liner-type spectra (Laing et al. 1994). However, two FR Is are known which have either a Seyfert 1 spectrum: S5 2116+81 (Lara et al. 1999) or a Seyfert 2 spectrum: PKS 2014−55 (Jones & McAdam 1992; Simpson et al. 1996); to the best of our knowledge, these are the only known cases. The other FR I emission line nebulae are extended (∼5 kpc) (Carrillo et al. 1999); the emission lines are weak; the emission line luminosity does not correlate with the radio luminosity (Zirbel & Baum 1995).

There are no obvious differences between the emission line spectra of radio quiet E galaxies, LERGs and most FR Is; FR I and radio quiet E galaxies of the same optical magnitude produce similar line luminosities (Sadler et al. 1989; Zirbel & Baum 1995).

4.4. Blazars

Blazars have been defined as extragalactic objects characterized by rapid optical variability, high optical polarization, large X-ray and γ-ray luminosities and a variable, flat-spectrum, superluminal radio core. The class of blazars includes the BLLs which have no or weak emission lines and the HPQs with strong, broad emission lines similar to those of normal QSOs.

The spectral energy distribution of BLLs discovered in X-ray and radio surveys differ significantly, leading to the subclassification of BLLs into X-ray selected and radio-selected objects (XBLs and RBLs respectively); this has subsequently been supplanted by a new classification "High energy peaked BLLs" (HBLs) and "Low energy peaked BLLs" (LBLs) (Giommi et al. 1995). Generally, XBLs tend to be HBLs and exhibit less extreme properties than RBLs which are usually LBLs. Studies of statistically complete samples of BLLs show that the observed dichotomy between XBLs and RBLs is an observational bias (Perlman et al. 1998; Laurent-Muehleisen et al. 1999).

Many of the observed properties of blazars can be reasonably understood if they are interpreted to be radio galaxies with their relativistic jet pointing toward us, BLLs and HPQs being associated with FR Is (or LERGs) and FR IIs respectively.

PKS 1413+135 is a puzzling object; while all other known BLLs have been found to be hosted by normal E galaxies (Scarpa et al. 1999), it is in an edge-on spiral (M^{c}Hardy et al. 1994) with a heavily obscured nucleus (Stocke et al. 1992).

4.4.1. Emission line properties

BLLs have been defined as blazars with rest-frame emission line equivalent widths smaller than 5Å (Morris et al. 1991; Stickel et al. 1991). Many authors have criticized this definition as being arbitrary. Burbidge & Hewitt (1987; 1992) have remarked that, when emission lines are detected in BLLs, they fall into one of two categories: they are broad, but weak, similar (except for their equivalent width) to those seen in normal QSOs, or they are weak and narrow such as [O II]λ3727, Hα, etc; they have suggested that objects in the first category are HPQs rather than genuine BLLs. The distribution of the Mg II EW in blazars is not bimodal (Mg II is the line most often observed in BLLs, see tables 3 and 4); there is continuity between objects with EW $>$ 5Å and those with EW $<$ 5Å (Scarpa & Falomo 1997); moreover there are objects that cross the boundary depending on the strength of their variable continuum (Antonucci et al. 1987).

In optically selected and lobe-dominated radio loud QSOs, *i.e.* in objects with no Doppler boosting, the luminosity of Hβ is closely proportional to the observed continuum luminosity with the median rest Hβ EW equal to 80Å while the Hβ luminosity varies by three orders of magnitudes (Miller et al. 1992); the median Mg II EW is $\sim$ 35-50Å (Steidel & Sargent 1991; Francis 1993). HPQs are most probably normal radio QSOs in which an intrinsically weak nuclear continuum source is strongly beamed due to the alignment of the nuclear jet with the line of sight; when the enhancement of this jet component is such that its apparent luminosity is equal to the unbeamed luminosity of the QSO accretion disk, the emission line equivalent widths are reduced by a factor of 2; but we cannot exclude the possibility that the enhancement factor in some of these objects is five to ten times larger or more reducing the mean value of the Mg II EW to less than 5Å; some of these objects would have no detectable broad emission lines and be called BLLs; however their extended radio luminosity would still be high.

We have seen above that, except for a single exception, none of the known FR I radio galaxies have broad emission lines implying that blazars which display broad emission lines, even with small EW, are HPQs rather than BLLs. On the other hand, many FR II radio galaxies have emission lines of very low excitation (the LERGs); they must be the parent population of a beamed subpopulation which would be optically similar to BLLs but would have relatively high extended radio luminosity (Laing et al. 1994; Wall & Jackson 1997).

BLLs are dominated by a bright compact radio core; but maps made with a high dynamic range often show an extended structure. If BLLs are FR Is with their jet pointing towards us, these extended radio structures should have the low luminosity typical of FR Is. However, a number of objects classified as BLLs have extended radio luminosities above the FR I/FR II division and could be misclassified FR IIs, *i.e.* HPQs (Cassaro et al. 1999).

There are 35 known objects often classified as BLLs and in which one (or more) broad emission line (C IV, Mg II, Hβ or Hα) has been detected; they are listed in tables 3 and 4; the 5 GHz luminosity (col. 7) is computed from the published values of the extended flux densities assuming a spectral index α=0.7.

Table 3. BLLs tentatively reclassified as HPQs (BL/HPQs). Col. 1: name, col.2: short position, col. 3: redshift, col. 4: HP indicates highly polarized QSOs, cols. 5 and 6: observed broad line and its rest EW, col. 7: 5 GHz luminosity of the extended component.

Name	Position	z			$EW_{\rm rest}$	$\log(L_{5GHz})$
PKS 0139−09	0138−09	0.733	HP	Mg II		25.4
3C 66.0A	0219+42	0.444?	HP	Mg II?		26.6
AO 0235+164	0235+16	0.940	HP	Mg II	<1.6-8	25.8
PKS 0537−441	0537−44	0.896	HP	Mg II	1.2-10	26.5
PKS 0754+100	0754+10	0.66	HP	Mg II?		24.9
PKS 0820+22	0820+22	0.951	HP	Mg II	4.9	26.3
PKS 0823+033	0823+03	0.506	HP	Mg II	5.1	24.3
0846+51W1	0846+51	1.860	–	C IV		-
OJ 287	0851+20	0.306	HP	Hβ	0.8	24.5
S5 0954+65	0954+65	0.367	HP	Hα	1.9	24.6
S5 1053+81	1053+81	0.706	–	Mg II		-
PKS 1144−379	1144−37	1.048	HP	Mg II	2.5	-
3C 279	1253−05	0.538	HP	Mg II	3.4	27.2
PKS 1335−127	1335−12	0.539	HP	Mg II	5.2-9.3	-
PKS 1514+197	1514+19	1.07	HP	C III		24.7
4C 14.60	1538+14	0.605	HP	Mg II	0.8	26.0
B2 1722+40	1722+40	1.049	–	Mg II	4.4	-
OT 081	1749+09	0.320	HP	Hβ	2.6-8	-
S5 1803+78	1803+78	0.684	–	Mg II	2.9	25.8
4C 56.27	1823+56	0.664	HP	Hβ	4.1	26.6
OV−236	1921−29	0.352	HP	Mg II	5.2	-
PKS 2029+121	2029+12	1.215	–	Mg II	4.9-8	-
PKS 2032+107	2032+10	0.601	HP	Mg II		25.5
PKS 2131−021	2131−02	1.285	HP	Mg II?		26.5
BL Lac	2200+42	0.068	HP	Hα	5.6-7.5	23.5
PKS 2240−260	2240−26	0.774	HP	Mg II	1.1	26.6

Many of these objects have a luminosity well above the FR I/FR II limit ($\sim 10^{32}$ erg s^{-1} Hz^{-1} at 5 GHz). The nine objects in table 4 show relatively strong (EW > 10Å) broad emission lines; we shall consider them in what follows as genuine HPQs. It is very likely that all the 26 objects in table 3 are also misclassified HPQs (we shall provisionally call them below BL/HPQs).

4.4.2. Brightness temperature and variability of the core

Kellermann et al. (1998) have used the Very Long Baseline Array at 15 GHz to image the structure of 132 strong compact AGNs, including 15 BLLs, 12 BL/HPQs and 31 HPQs, and derived the maximum brightness temperatures T (all T's listed in their table 3 are low by a factor of ten; Kellermann (1998), private communication). Many of the measured angular diameters are not larger than the nominal resolution, therefore the derived brightness temperatures are often lower limits.

Möllenbrock et al. (1996) have observed with VLBI at 22 GHz 140 compact extragalactic radio sources, including 14 BLLs, 11 BL/HPQs and 42 HPQs. Meaningful values of the brightness temperature have been obtained for 9 BLLs, 9 BL/HPQs and 32 HPQs.

Table 4. BLLs with strong broad emission lines (EW > 10Å), reclassified as HPQs. Col. 1: name, col. 2: short position, col. 3: redshift, col. 4: HP indicates highly polarized QSOs, cols. 5 and 6: observed broad line and its rest EW, col. 7: 5 GHz luminosity of the extended component.

Name	Position	z			EW_{rest}	$\log(L_{5GHz})$
PKS 0057−338	0057−33	0.875	–	Mg II	9.8	-
PKS 0215+015	0215+01	1.721	HP	C IV	13.2	26.7
PKS 0256+075	0256+07	0.893	HP	Mg II	24.1	26.4
PKS 0306+102	0306+10	0.863	–	Mg II	35.0	-
PKS 0521−36	0521−36	0.055	HP	Hα	26.2	25.7
B2 1308+32	1308+32	0.997	HP	Mg II	19.0	25.8
3C 446	2223−05	1.404	HP	Mg II	16.2	-
3C 454.3	2251+15	0.859	HP	Mg II	20.0	27.1
S5 2353+81	2353+81	1.334	–	Mg II	27.0	-

Fig. 6 shows the histograms of the observed brightness temperatures for the BLLs, BL/HPQs and HPQs separately for the two samples. It appears that the distributions of brightness temperatures are significantly different for BLLs and HPQs and that the distribution for the BL/HPQs is very similar to that of the HPQs. In fact, on average, the brightness temperatures for BL/HPQs are slightly higher than those of HPQs, in agreement with the assumption that BL/HPQs are extreme cases of HPQs with, on average, larger boosting factors.

Lähteenmäki & Valtaoja (1999) have used 22 and 37 GHz continuum flux data to derive variability time-scales and associated brightness temperatures T for a sample of 25 HPQs, 11 BL/HPQs and 10 BLLs. The variability time-scale is defined as $\tau = dt/d[ln(S)]$ (Burbidge et al. 1974). Again, the brightness distribution of the BL/HPQs is much more similar to that of the HPQs than to that of the BLLs: the brightness temperatures of the 7/9 BLLs are lower than $3\,10^{12}$ K; on the other hand, only 1/25 HPQ has such a low T, while 3/11 BL/HPQs have a low T.

The brightness temperatures derived from variability are systematically larger than those obtained directly from VLBI measurements because of the different dependence on the Doppler factor: $T_{VLBI}=T_o\ \delta$ and $T_{var}=T_o\ \delta^3$, *i.e.* $T_{var}=T_{VLBI}\ \delta^2$ (Lähteemäki et al. 1999).

Readhead (1994) and Lähteenmäki et al. (1999) showed that the maximum intrinsic brightness temperature is the equipartition value $\sim 5\,10^{10}$ K rather than the inverse Compton value $\sim 10^{12}$ K. Lähteenmäki & Valtaoja (1999) computed the boosting Doppler factor using the equation: $\delta=(T/10^{10.7})^{1/3}$ (Blandford & Königl 1979); they found that generally the BLLs have a Doppler factor $\delta < 3$ (except for OJ 425, PKS 1413+135 and S5 2007+77), while for HPQs and BL/HPQs, δ is in the range 4-25.

Hughes et al. (1992) have made a structure function analysis of the total flux density at centimeter wavelengths of 51 core dominated objects, including 12 BLLs, 6 BL/HPQs and 12 HPQs; they estimated a characteristic time-scale of variability (in the observer's frame) for each object; the distributions for the BL/HPQs and the HPQs are similar, while the distribution for the BLLs is significantly different; the median value is $\sim$ 1 yr for both BL/HPQs and HPQs; it

is $\sim$ 3 yr for BLLs. There are 4/12 BLLs, 5/6 BL/HPQs and 10/12 HPQs with a time-scale smaller than 2.5 year. The one BLL with a very small time-scale (log(t)=$-$0.5) is PKS 0048$-$09.

Smith & Nair (1995) have determined the rest-frame time-scale of variation of the base level of the optical light-curve of a sample of 36 BLLs; they found that objects with z $>$ 0.4 (*i.e.* basically what we call BL/HPQs) have a mean rest-frame time-scale of 2.42 yr, while the mean time-scale for objects with z $<$ 0.4 is 6.61 yr.

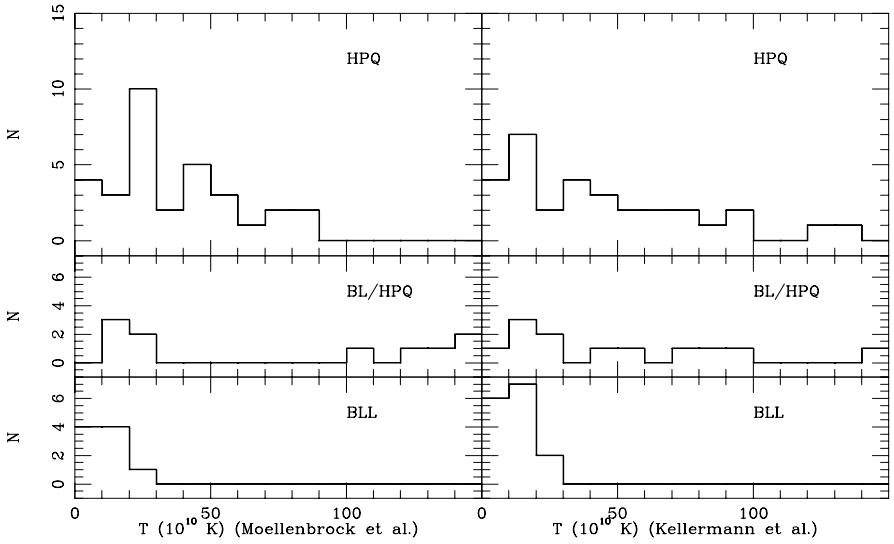

Fig. 6. Distributions of the brightness temperature of blazar radio cores as measured by Möllenbrock et al. (1996) and Kellermann et al. (1998)(after correction by a factor of ten; see text), plotted separately for the HPQs, BL/HPQs and BLLs.

Heidt & Wagner (1996) have studied the optical intraday variability of 26 objects from a complete sample of 34 BLLs. The activity parameter I (in % per day) shows a bimodal distribution; eleven objects display an I between 3 and 27, while 15 have I $<$ 3. Twelve of these objects are BL/HPQs, seven having I $>$ 3, while only 4/14 BLLs have such a high variability index. There is therefore a correlation between fast optical variability and the presence of broad emission lines. The four BLLs with I $>$ 3 are: PKS 0426$-$380 and S4 1749+70 which both have a high luminosity extended radio component (see table 5), S5 0716+714 and OQ 530. Heidt & Wagner have noted that low redshift (z $<$ 0.4) objects have on average lower values of I than high z objects which is a similar effect since high z BLLs either have broad emission lines or may be extreme cases of HPQs with a very high amplification of the featureless continuum.

51 AGNs, all flat spectrum radio sources, including 7 BLLs, 7 BL/HPQs and 13 HPQs, are known to be sources of high-energy γ-rays (100 MeV). 77% (10/13) of the HPQs are variable in γ-rays while 71% (5/7) of the BL/HPQs and 28% (2/7) of the BLLs (S5 0716+71 and PKS 2155−304) are variable (Mukherjee et al. 1997).

It is clear that BLLs have lower brightness temperatures and are less variable on the average than both HPQs and BL/HPQs.

4.4.3. Doppler and Lorentz factors

Ghisellini et al. (1993) have derived a lower limit of the Doppler factor δ for a sample of 19 BLLs, 13 BL/HPQs and 24 HPQs from the condition that the synchrotron self Compton flux should not exceed the observed flux at high frequencies. They found that the δ distribution for BLLs and HPQs are significantly different, with BLLs having lower values of δ. 19/24 HPQs have $\delta > 5$, while only 3/19 BLLs have such a high value of δ (PKS 0048−09, PKS 0735+17 and PKS 1519−27); 8/13 BL/HPQs have $\delta > 5$.

The equipartition Doppler factors are derived assuming that the sources are at or near equipartition of energy between radiating particles and magnetic field (Readhead 1994). Güijosa & Daly (1996) have computed the equipartition Doppler factor for the objects in the Ghisellini et al. sample. They found that 5/19 BLLs have $\delta > 2$, while 10/13 BL/HPQs and 18/23 HPQs have such a large value of δ.

Comparisons between the inverse-Compton and equipartition Doppler factors shows a high correlation between the two estimates, suggesting that they are both reliable (Güijosa & Daly 1996; Fujisawa et al. 1999).

Fig. 7 shows the distributions of the Doppler factors for BLLs, HPQs and BL/HPQs as derived by the two methods. Again, we find that weak broad line objects are more similar to HPQs than to objects with no detected broad lines.

The apparent transverse velocity of a moving feature is $\beta_a = \frac{\beta\, sin\theta}{1-\beta\, cos\theta}$. The maximum transverse velocity for a given value of β is $\beta_a = \beta\gamma$ (which is larger than 1 when $\beta > 2^{-0.5}$) or $\beta_a \sim \gamma$ when $\beta \sim 1$. Gabuzda et al. (1994) have shown that the typical VLBI component apparent speed β_a in BLLs are systematically lower than those in HPQs. To get this result, they used measurements of 12 BLLs. Five of these objects have been reclassified as BL/HPQs; the difference between the two distributions becomes even more striking, the median values of β_a being 4 and 9 for the BLLs and the HPQs respectively. The BLL Mark 421 has no superluminal motion which could arise if the source is aligned almost exactly (within 0.4°) with the line of sight (Piner et al. 1999).

Several authors have estimated the mean value of R, the ratio of the compact-to-extended radio luminosity, for the RBLs; they found that it is much larger than for FR Is (Padovani 1992; Perlman & Stocke 1993; Maraschi & Rovetti 1994; Kollgaard et al. 1996); the estimates of the ratio of the mean R values for BLLs to that for FR Is range from 200 to 4 000; if this is taken as the mean

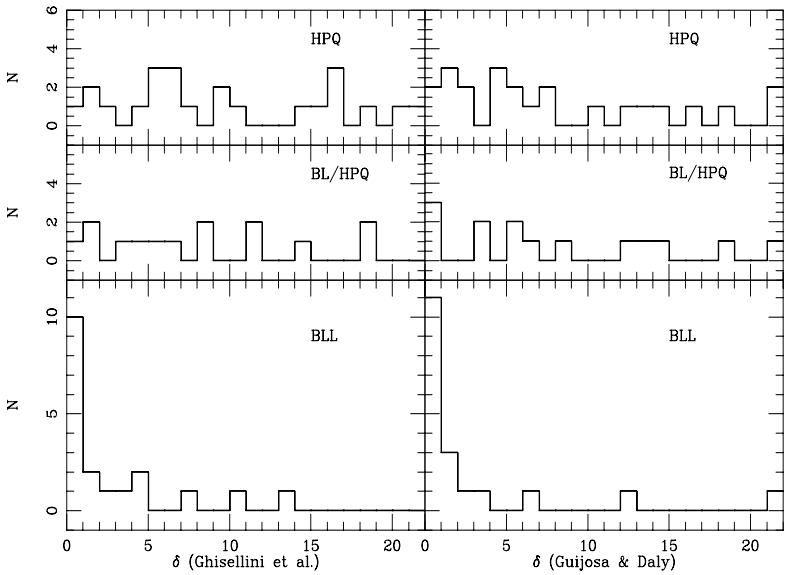

Fig. 7. Distributions of blazar Doppler factors determined in two different ways by Ghisellini et al. (1993) and by Güijosa & Daly (1996), plotted separately for the HPQs, BL/HPQs and BLLs.

value of R/R_0, it indicates values of γ in the range 3-6 if p=2. According to Maraschi & Rovetti (1994), the distribution of R for BLLs and HPQs are undistinguishable; however, as the mean value of R is larger for FR Is than for FR IIs sources, it follows that R_0 is on average larger for BLLs than for HPQs, implying a smaller average value for γ.

Again, we find that BL/HPQs have Doppler and Lorentz factors more similar to HPQs than to BLLs.

A weak unresolved optical nuclear source has been detected with the *HST* in the great majority (85%) of a complete sample of 33 FR I galaxies, the luminosities of the optical and radio cores being strongly correlated. The detection of a compact optical core in most FR Is indicates that we have a direct view of the innermost regions and that the obscuring torus, if any, must be very thin; the correlation between the luminosities of the optical and radio cores suggests that the optical core is emitted by the jet itself rather than by a weak accretion disk (Chiaberge et al. 1999).

The luminosities of the optical cores found in FR I radio galaxies are $2\,10^2$ to $3\,10^5$ times weaker than the core luminosity of BLLs selected for having similar host galaxy magnitude and extended radio luminosity, suggesting that BLLs are optically dominated by the beamed radiation from a relativistic jet with Lorentz factor $\gamma \sim$ 5-10 (Capetti & Celotti 1999); this range of values is significantly larger than the range obtained from radio data!

4.4.4. The dual nature of the BLLs

Our analysis of the published results confirms the assumption made by a number of authors that the sources classified as BLLs are a mixture of two physically different populations with different parent objects. One population consists of sources which are closely aligned with our line of sight and have large Lorentz factor ($< \gamma > \sim 10$); they are highly variable and have high brightness temperatures; they are the extreme end of the HPQ population with the smallest viewing angles; their parent population is the strong, distant FR II radio galaxies. The other population consists of sources which are also beamed toward us, but not as closely as the "distant BLLs"; they have smaller Lorentz factor ($< \gamma > \sim 3$) and consequently have smaller brightness temperatures and are less variable; they are FR I radio galaxies favorably oriented. Kollgaard (1994), using various methods, obtained a slightly larger value ($< \gamma > \sim 4$) which may be due to the fact that his sample of BLLs was contaminated by the presence of some miss-classified HPQs having larger values of γ.

The inclusion of a sizable number of HPQs in samples of BLLs may lead to incorrect conclusions.

Stickel et al. (1991) have used their complete sample of 34 BLLs to build their core radio luminosity function at 5 GHz. Urry et al. (1991) have compared this luminosity function to that of FR Is; they found that the space densities of BLLs and FR Is are about equal above 10^{33} erg s^{-1} Hz^{-1}, the space density of BLLs being about 30 times smaller than that of FR Is below 10^{32} erg s^{-1} Hz^{-1}. However, the BLL radio luminosity function was built assuming that the 34 objects in the sample were genuine BLLs; but we have reclassified as HPQs 16 of these objects and 10 more could be HPQs.

Table 5. BLLs in the Stickel et al. (1991) complete sample, with no measured redshift or with z > 0.4. Col. 1: name, col. 2: position, col. 3: redshift, col. 4: HP indicates highly polarized QSOs, col. 5: 5 GHz luminosity of the extended component.

		z		$\log(L_{5GHz})$
PKS 0048−09	0048−09		HP	25.8
PKS 0118−272	0118−27	>0.557	HP	>25.8
PKS 0426−380	0426−38	>1.030	–	>25.5
S5 0454+84	0454+84	>1.340	HP	-
S5 0716+71	0716+71		HP	26.2
PKS 0735+17	0735+17	>0.424	HP	>25.5
OJ 448	0828+49	0.548	HP	-
B2 1147+24	1147+24		HP	25.4
PKS 1519-273	1519−27		HP	25.1
S4 1749+70	1749+70	0.770	HP	25.5

Stickel et al. (1991) sample contains 10 objects with no measured redshift or with z > 0.4 (table 5). Most objects with no measured redshift probably have a relatively high z (>0.5) since, in general, it has not been possible to detect the host galaxy (Kotilainen et al. 1998). We have computed the extended radio luminosity of these 10 objects assuming that the redshift is z=0.5 when it was not known. It seems very likely that at least eigth of them are extreme cases of HPQs. Indeed, most have a rather high extended radio luminosity; PKS 0048−09,

PKS 0735+17 and PKS 1519−27 have a high δ (> 5); PKS 0426−380, S5 0716+71 and PKS 1749+70 have a high index of rapid optical variability (I > 7.7 %); PKS 0735+17 and PKS 1749+70 show high superluminal velocities (β_a > 6c). The status of two objects (S5 0454+84 and B2 1147+24) is rather uncertain due to the lack of data; they could possibly be genuine BLLs.

We are then probably left with only 8 to 10 genuine BLLs; their luminosity function is therefore very poorly determined, especially for luminosities larger than 10^{32} erg s^{-1} Hz^{-1}; in fact, we cannot exclude that the space density of BLLs is 30 times smaller that of FR Is for any value of the radio luminosity. Owen et al. (1996) expected to find 3 BLLs out of 18 observed FR Is with radio luminosities > 10^{32} erg s^{-1} Hz^{-1}; they found none. This result is not in contradiction with the corrected BLL luminosity function.

Urry et al. (1999) have observed the host galaxies of nine BLLs with the *HST*; one has no reliable measured redshift and three have been reclassified as HPQs. The host galaxy has been detected in each of the five remaining BLLs ; they are E galaxies with smooth morphology; their average k-corrected absolute magnitute is −23.6 (rather than −24.6 as given by Urry et al. for the seven detected objects). This again stresses the need of a good classification of all objects in a sample to get reliable results.

4.5. Basic differences between FR Is, FR IIs and radio quiet AGNs

4.5.1. Radio loud *vs.* radio quiet AGNs

What is the difference between E and spiral galaxies that is relevant to making active nuclei produce radio jets often in one, never in the other?

There is a very limited range of inputs that determine the nature of an AGN: the fuel supply, the mass of the BH and its angular momentum. The fuel supply rate is similar for AGNs in radio-loud and radio-quiet objects since both cover the whole range of luminosities; regarding the mass of the BH, the Eddington limit indicates that masses up to 10^8 $M_\odot$ occur in some radio-quiet AGNs; somewhat more massive BHs could occur in radio galaxies, but masses in excess of 10^{10} $M_\odot$ seem to be ruled out on dynamical grounds, at any rate in the nearest gEs; the difference between E and spiral galaxies should then be the larger angular momentum of the central BH in E galaxies (Blandford 1990; Scheuer 1992).

Blandford (1990) argued that sub-Eddington mass accretion rates produce slowly spinning BHs and that rapidly spinning BHs require high accretion rates. However, in FR Is objects, the accretion rates are certainly small and yet these objects have a radio jet implying a rapidly rotating BH; moreover NLS1s are generally radio quiet spiral galaxies which are believed to contain a small mass BH accreting matter at a high rate. Therefore, the larger angular momentum of the central BH in E galaxies is more probably the result of the merging of two BHs (Scheuer 1992).

Until about 1975, it was commonly assumed that E galaxies were rotationally flattened and oblate; however, the first accurate measurements of the rotation velocities of E galaxies revealed a significantly lower rotation rate than

expected; E galaxies were shown to be "hot" stellar systems in which most of the support against gravitational collapse comes from essentially random motions, rather than "cold" systems like spiral galaxies in which ordered rotation contributes most of the internal kinetic energy. One model for the formation of E galaxies that has gained many adherents is the merger hypothesis proposed by Toomre & Toomre (1972). According to this hypothesis, most or all E galaxies formed from the coalescence of spiral galaxies. Evidence in favor of the merger hypothesis include the discovery of a number of fine structure features such as ripples, twists, imbedded disks and tidal tails (Merritt 1993); many, perhaps all, gE galaxies have galactic cluster systems that show bimodal metallicity distributions generally attributed to merging (Côté et al. 1998; Kissler-Pattig et al. 1998). It seems now clear that E galaxies include some objects formed by fairly recent mergers of disk systems (Barnes 1999). The kinematic and photometric properties of luminous IR merging galaxies are consistent with their evolving into E galaxies; gE galaxies, if they are formed through mergers, probably evolve from ULIGs (Shier & Fischer 1998).

Compact dark masses, probably massive BHs, have been detected in the core of many normal galaxies using stellar dynamics (Kormendy & Richstone 1995). The massive BH mass appears to correlate with the galactic bulge luminosity, with the BH being about one per cent of the mass of the spheroidal bulge (Franceschini et al. 1998; Magorrian et al. 1998; Richstone et al. 1998; van der Marel 1999). This relation is similar to the one found for QSOs (Laor 1998). The observed relation between BH masses and bulge masses can be reproduced if the mass accreted during a major merger is a fixed fraction of the mass of the gas that has formed stars in the merging galaxies since the last major merger (Cattaneo et al. 1999).

Indirect evidence for binary orbital motion may be present in the wiggles of a milliarcsecond radio jet (Roos et al. 1993). Sillanpää et al. (1996),Villata et al. (1998) and Sundelius et al. (1997) showed that the optical light curve of OJ 287 features repeated outbursts at $\sim$12 yr intervals suggesting that it contains two supermassive BHs in a binary system (SMBBH) with a (rest-frame) orbital period of 8.9 yr. This prompted Sillanpää (1999) to suggest that, in radio quiet objects, there is a single supermassive BH in the nucleus of the host, but in the radio loud objects, there is a SMBBH.

When two galaxies containing a nuclear BH merge, the two BHs form a binary and may eventually coalesce (Begelman et al. 1980). For Wilson & Colbert (1995), galaxies which have not suffered a major merger event contain a non-rotating or a slowly rotating BH; if the two BHs have roughly equal mass, a rapidly spinning BH will result; such mergers could be the progenitors of powerful radio sources in which the radio jets are powered by the spin energy of the merged hole (Blandford 1999). The spindown time due to this loss of energy is much shorter than the Hubble time and consequently the life-time of radio loud AGNs is short and these AGNs should be the result of recent mergers (Meier 1999).

More and more facts support the idea of a dichotomy in E galaxies which can be divided into "disky" and "boxy" objects from isophotal analy-

sis (Nieto & Bender 1989); boxy Es are bright and rotate slowly, disky Es are weak and rotate rapidly; radio loud Es have been found to be boxy; disky Es are mostly radio quiet (Bender et al. 1989; Kormendy & Bender 1996). However, the cause of the differences between disky and boxy galaxies is not yet understood. Kissler-Patig et al. (1998) suggested that disky Es have kept their original structure while boxy Es are the result of merger. Faber et al. (1997) proposed that disky Es were formed in gas-rich mergers and boxy Es in gas-poor mergers but, for Naab et al. (1999) merging of two equal-mass spirals leads to an anisotropic, slowly rotating system with preferentially boxy isophotes, while unequal-mass mergers result in the formation of rotationally supported Es with disky isophotes.

4.5.2. FR I *vs.* FR II radio galaxies: the ADAF model

The ADAF model

It is believed that most gE galaxies possess a nuclear BH with a mass in excess of 10^8 $M_\odot$. Bondi accretion from the interstellar medium might then be expected to produce quasar-like luminosities from the nuclei of most gE galaxies. It is a puzzle that such luminosities are not observed (Fabian & Canizares 1995). Motivated by this problem, Fabian & Rees (1995) have suggested that the final stages of accretion in these objects occur in an advection dominated accretion flow (ADAF) with a small radiative efficiency.

ADAFs occur when the local cooling time-scale becomes longer than the accretion time-scale so that most of the dissipatively liberated energy is advected inward with the accreting gas and lost into the BH. The viscous heating is assumed to affect mainly the ions, while the radiation is produced primarily by the electrons; as the ions transfer only a small fraction of their energy to the electrons via Coulomb collisions, the radiative efficiency of an ADAF is much less than the total energy released during accretion. The result is that the ion temperature becomes almost virial ($T\sim10^{12}$ K) which causes the flow to have a nearly spherical morphology; the electron temperature is determined by a balance between heating due to collisions with the ions and inverse Compton cooling and reaches T_e $\sim10^9$-$10^{9.5}$ K. This happens for accretion rates below $\dot{M}_{crit}\sim \alpha^2$ $\dot{M}_{Edd}$, where α is the viscosity parameter and $\dot{M}_{Edd}$ is the accretion rate corresponding to the Eddington limit. If $\alpha = 0.1$ then advection can dominate the flow if the accretion proceeds at less than 1% of the Eddington rate. For such low accretion rates, the expected luminosity scales as $\dot{M}^2$ rather than $\dot{M}$ and the luminosity of the system falls well below the luminosity which is normally expected from accretion (Narayan et al. 1999; Mahadevan 1999). It is often assumed that there is, in these objects, an outer region extending outward from about 3 000 Schwarzschild radii where the accretion flow is in the form of a standard geometrically thin disk (Narayan et al. 1999).

The entire spectrum of an ADAF is completely determined by the mass of the BH and by the value of the transition radius out of which the disk is thin; it is very characteristic: a $\nu^{1/3}$ slope in the radio regime, a submillimeter-to-X-ray Compton spectrum, and a hard-X-ray-to-γ-ray Bremsstrahlung spectrum

(Mahadevan 1997).

The radio emission is due to cyclo-synchrotron radiation from hot electrons in the equipartition magnetic field; it should be isotropic. In the absence of a radio jet, the expected core radio luminosity is relatively low and roughly proportional to the mass of the central BH; the 5 GHz ADAF luminosity is L $(=\nu\ L_\nu) < 10^{38}$ erg s^{-1} for $M_{BH} < 10^9\ M_\odot$; however, some level of jet activity not directly associated with the ADAF seems to be present in most sources and the observed radio emission can be considerably larger (Fabian & Rees 1995; Yi & Boughn 1999). Di Matteo et al. (1999) have shown that the high frequency radio emission of the nucleus of the gE galaxies for which the mass of the central BH has been estimated is significantly lower than predicted by the ADAF model, suggesting not only that there is no radio jet in these objects but also that that the radio emission due to the ADAF is being suppressed.

FR I *vs.* FR II radio galaxies

The differences in the large-scale properties of FR Is and FR IIs radio sources are most probably related to both intrinsically different core properties (Lorentz factor, accretion rate etc) and differences in the environment outside the nuclear region of the associated optical galaxy (Venturi et al. 1995; Pearson 1996; Giovannini et al. 1996). This would explain why there is no exact correspondence between high- and low-ionization objects (governed by the properties of the core) and their radio morphology which depends both on the "strength" of the jet and the density of the environment.

Radio loud AGNs are basically similar to their radio quiet counterparts, except for the presence in the former of a radio jet which is generally attributed to the effect of a rapidly rotating BH. The rotation rate of the BH seems therefore to have no influence on the other observable properties of the AGNs. If FR Is and FR IIs were differing only by the spin rate of their BH, they would differ by the properties of their jets, not by those of their optical nuclei.

It is customary to assume that the accretion power is radiated away with an efficiency $\simeq$0.1 close to the surface of a BH; in other words, it is assumed that most of the gravitational energy released through viscous dissipation is radiated away locally from the accretion disk; this condition is very well satisfied for a geometrically thin accretion disk.

It seems now well established (see above) that FR Is and BLLs have jets which are relativistic near to the nucleus but with Lorentz factors systematically smaller than in FR IIs and HPQs. According to Appl & Camenzind (1993) and Blandford (1994), this difference could be due to the fact that FR II jets arise from a nucleus with a rapidly rotating BH, and FR I jets from a nucleus with a slowly rotating BH. Alternatively, it could be the result of different jet collimation mechanisms associated with an accretion flow of a different nature (Baum et al. 1995).

While supplying large power to their radio emitting regions, the nuclei of FR I radio galaxies emit little detectable radiation; however, the total energy content of the extended radio components implies that the galaxy nucleus contains a BH of mass 10^7-10^8 $M_\odot$; this suggests that their center contains a spinning BH surrounded by an ADAF; the thick disk anchors magnetic fields which extract rotational energy from the hole in the form of two collimated beams of relativistic particles and magnetic fields; these, in turn, drive the observed radio jets (Rees et al. 1982).

The main difference between FR Is and FR IIs (more specifically between low and high-excitation galaxies) would be that the accretion rate is small in the former and that, consequently, the accretion flow is advection dominated (Baum et al. 1995; Reynolds et al. 1996).

It has been suggested that the FR I galaxy M 87 and the weak radio galaxy NGC 4649 which, despite possessing evidences for a supermassive BH, have a very low core luminosity, contains an ADAF (Reynolds et al. 1996; Di Matteo & Fabian 1997).

AGN-type Liners and ADAFs

It is natural to assume that the basic difference between Liners and Seyferts is the same as between FR Is and FR IIs. Indeed, Lasota et al. (1996) suggested that the parameter that distinguishes Liners from Seyferts is their small L/L_{Edd} and that their accretion flow is advection dominated. For Yi & Boughn (1999), Liners with both X-ray and high-frequency radio fluxes have ratios of radio to X-ray luminosities compatible with being due to an ADAF.

Sambruna et al. (1999) have found in five out of six LERGs a hard X-ray component of low luminosity ($L_{2-10keV} \sim 10^{40}$-10^{42} erg s^{-1}) suggesting that indeed they are low accretion rate AGNs powered by an ADAF.

Liners tend to show little or no significant short-term X-ray variability; this is a marked break from the trend of increased variability in Seyfert 1s with lower luminosity; this difference could be due to the presence of an ADAF resulting in a larger characteristic size for the X-ray producing region than in the case of Seyferts (Ptak et al. 1998).

We have seen above (sec. 2.1.2) that a small number of AGNs have double-peaked broad line profile and that these objects have a Liner-like narrow line spectrum. Chen & Halpern (1989) showed that, although a Keplerian disk fits the line profiles of these objects, a cool thin accretion disk does not account for the line fluxes; they propose that, in these cases, a thick, hot ion torus occupies the inner disk and that inverse Compton scattered X-rays from the torus illuminate a thin outer disk. In the spectra of these objects, the fraction of starlight is significantly larger than in the spectra of "classical" BLRGs; in BLRGs, the thermal blue/UV component which is commonly attributed to the inner parts of an optically thick accretion disk is easily observed; if the inner disk is replaced by an ion torus, the blue/UV bump should disappear which seems to be the case

in the double-peaked objects (Eracleous & Halpern 1994). This is additional evidence for the presence of an ADAF in Liners; but it has not yet been shown that the continuum emitted by ADAFs could produce a Liner-like spectrum.

The presence of water megamasers in Seyfert 2s proves the existence in these objects of a molecular torus. The H_2O emission lines in NGC 1052, a FR I radio galaxy, are relatively broad and smooth, unlike the narrow maser spikes seen in Seyfert 2s; the masers lie along, rather than perpendicular, to the jet and there is no indication of the existence in this object of an accretion disk (Claussen et al. 1998).

NGC 1052 is an FR I; a broad Hα component (2 120 km s^{-1} FWHM) is visible in total light; in polarized light, there is a significantly broader (4 920 km s^{-1} FWHM) component which is most probably due to scattering by electrons in a medium with $T_e \sim 10^5$ K. It seems therefore that the nucleus is seen directly (Barth et al. 1999a). However, Guainazzi & Antonelli (1999) and Weaver et al. (1999) have observed NGC 1052 in X-rays; they found that the most convincing model is a nuclear source obscured by a screen of matter with column density $\sim 10^{23}$ cm^{-2}. Such a high column density of cold matter would completely obscure the optical nucleus.

Barth et al. (1999b) have recently discovered the presence of broad polarized Hα emission in the spectrum of two additional Liners, both hosted by a FR I galaxy (NGC 315=B2 0055+30, and NGC 4261=3C 270.0) (Mack et al. 1997; Morganti et al. 1993).

We have seen that the presence of double-peaked broad emission lines in Liners has been tentatively interpreted as emission from an external thin disk heated by the radiation of the internal hot thick torus; the weak broad lines observed in a number of Liners could be due to the same mechanism.

NGC 4258 has often been classified as a Liner; it is however a Seyfert 2 (Ho et al. 1997b); moreover, the presence of a molecular disk (Miyoshi et al. 1995) is unexpected in Liners. The mass of the central BH in NGC 4258 is $3.6\,10^7$ M$_\odot$ (Miyoshi et al. 1995); the Eddington luminosity corresponding to this mass is $L_{Edd}=4.5\,10^{45}$ erg s^{-1}; the bolometric luminosity has been estimated to be $L_{bol} \sim 3.4\,10^{42}$ erg s^{-1}, implying a sub-Eddington luminosity $L \sim 0.75\,10^{-3}$ L_{Edd}; it has therefore been suggested that the nucleus of NGC 4258 contains an ADAF (Lasota et al. 1996; Gammie et al. 1999; Chary et al. 1999). The low radio luminosity of the central engine however call into question the ADAF mechanism in this object (Herrstein et al. 1998), although radio luminosities lower than predicted may not be exceptional (Di Matteo et al. 1999).

To conclude, it seems that the difference between radio loud and radio quiet AGNs is that the BH in the former have a high spin rate. The difference between high- and low-ionization radio galaxies and between Seyferts and Liners is the low accretion rate in low-excitation objects resulting in the formation of these objects of a hot, optically thin, geometrically thick disk, while the Seyferts contain a cool, optically thick, geometrically thin disk. However although the ADAF model looks very promising, it should be stressed that no really convincing evidence exists for the presence of an ADAF in any AGN.

It appears that the main spectroscopic characteristic of the Liners is the low-ionization spectrum due to ionization by the emission of a very hot plasma, the thick inner torus, while Seyferts are ionized by the thermal UVX emission of a cool thin torus. Liners may have broad emission lines which however are weak compared to the narrow emission lines. This leads us to revise our classification of blazars: it is not the presence of broad emission lines which puts a blazar in the HPQ class, but the presence of broad lines associated with high-excitation narrow lines; unfortunately, as the EW of the lines in these objects is small, such a classification is rarely possible. However, the similarity we have found between the properties of BL/HPQs and HPQs suggest that only a small number of BL/HPQs could really be BLLs with a low-excitation narrow line spectrum. This may be the case for BL Lacertae itself as the spectrum published by Corbett et al. (1996) has strong [O I] and [N II] lines relative to the narrow component of Hα. Moreover, BL Lacertae has all the characteristics of the genuine BLLs: small radio brightness temperature, small amplitude of intraday optical variability and of γ-ray variability, small Doppler and Lorentz factors.

5. RED QSOs AND TYPE 2 QSOs

5.1. The relative number of Seyfert 1 and 2 galaxies

We have seen that Seyfert 1s are objects seen at a relatively narrow angle to the axis of the dusty torus, while Seyfert 2s are seen at larger angles such that the nucleus is hidden from view. In Seyfert 1.8s and 1.9s, the line of sight is more or less tangent to the torus and the nucleus is seen through a moderate amount of absorption. The determination of the relative number of Seyfert 1s to Seyfert 2s per unit volume would be a measurement of the covering factor of the torus, *i.e.* of its opening angle.

For many years Seyfert 1s, which were largely UV excess selected, were thought to outnumber Seyfert 2s. More recently, a number of studies of complete samples of bright galaxies have allowed to derive an estimate of the ratio of the space density of Seyfert 2s to Seyfert 1s. Simkin et al. (1980) and Véron & Véron-Cetty (1986) found that the space densities of Seyfert 2s and Seyfert 1s are about equal; Maiolino & Rieke (1995) found that the relative number of Seyfert 2s to Seyfert 1s is $\sim$1.5, while Phillips et al. (1983) and Huchra & Burg (1992) found that the space density of Seyfert 2s is approximately twice as large as the space density of Seyfert 1s. Osterbrock & Shaw (1988) obtained a space density about three times larger for Seyfert 2s than for Seyfert 1s.

The thermal infrared photons are emitted isotropically so that both Seyfert types should have the same IR luminosities. Lawrence et al. (1986) have identified 530 IRAS sources from a complete flux limited sample ($S_{60\mu m} > 0.5$ Jy), which contains 10 galaxies tentatively classified as Seyfert 1s and 17 which are most probably Seyfert 2s, giving a ratio of Seyfert 2s to Seyfert 1s $\sim$1.7. Veilleux et al. (1999), in a complete sample of 108 ULIGs making up an unbiased flux-limited ($S_{60\mu m} > 1$ Jy) infrared sample, have found 10 broad line and 23 narrow line AGNs so, in this case, Seyfert 2s outnumber Seyfert 1s by $\sim$2.3.

In a complete sample of 49 FR IIs, Hardcastle et al. (1998) have found 15 LERGs, 9 BLRGs and 25 NLRGs. Discarding the low-excitation objects, the proportion of NLRGs to BLRGs is ∼2.8.

Several bias could affect these results; in weak line objects, broad lines could escape detection while the narrow lines suggest a Seyfert 2; on the other hand, in magnitude limited samples, galaxies with a bright Seyfert 1 nucleus will be selected even if the parent galaxy is weaker than the magnitude limit of the sample.

All these studies give results which, although not in perfect agreement, are rather similar: the ratio of the volume density of Seyfert 2s to Seyfert 1s is probably somewhere between 1.5 and 2.

5.2. Red QSOs

If QSOs are high luminosity Seyfert 1s, high luminosity Seyfert 1.8s, 1.9s and 2s should exist (Wills 1999). Type 1.8 and 1.9 QSOs should appear as QSOs with a reddened continuum and a high Balmer decrement; they are called "red QSOs".

Most radio quiet QSOs have been discovered by UV-excess surveys which are biased against reddened QSOs. The identification of red QSOs suffers from a redshift bias in optical surveys because at higher redshifts optical spectra sample shorter wavelengths where there is greater extinction (Willott et al. 1998). Rowan-Robinson (1995) showed that UV-selected QSOs indeed suffer little extinction (0 to 0.55 mag.).

In radio loud QSOs, the optical continuum steepens and the narrow-line EWs and Balmer decrements of the broad-line components increase with increasing viewing angle (decreasing flux ratio R of the core to the extended radio components), implying that reddening is considerable ($A_V \sim$ 2-4 mag) in most lobe-dominated QSOs (Jackson & Browne 1991; Baker 1997); the broad lines are reddened more than the narrow lines, locating much of the dust responsible for absorbing the broad-line emission between the broad- and narrow-line regions (Hill et al. 1996; Baker 1997). Hα is the only broad line that has been detected in the two QSOs 3C 22.0 (Rawlings et al. 1995) and RX J1343.4+0001 (Shanks et al. 1996). All these objects are the QSO equivalent of Seyfert 1.8 and 1.9 galaxies.

Webster et al. (1995) discovered many sources with unusually red optical continua (B−K) among the QSOs of the Parkes sample of flat-spectrum radio sources and interpreted this result in terms of extinction by dust. They suggested that existing surveys of bright optical QSOs may be missing ∼80% of QSOs with a given intrinsic optical magnitude. Benn et al. (1998) showed that many of the reddest steep spectrum radio loud QSOs have non-stellar images in K, consistent with underlying gE galaxies, suggesting that contamination by starlight accounts for much of the reddening of the measured B−K colours for these objects; however, Masci et al. (1998) showed that this may not be the case for flat spectrum QSOs the colours of which could be explained by the addition

of a red synchrotron component to an underlying blue continuum which is identical to that in radio quiet QSOs.

X-ray selection is a way of finding red QSOs efficiently: hard X-rays (2-10 keV) penetrate even tens of magnitudes of optical extinction with minimal absorption; even the lower energy band of ROSAT (0.5-2.5 keV) is not strongly affected by optical extinction of up to ∼2 magnitudes. Kim & Elvis (1999) have looked for red starlike objects associated with ROSAT sources and found seven red QSOs; their Hα/Hβ ratio, optical slope and X-ray colours all indicate that they are absorbed by A_V ∼2 mag. Their spectra could be classified either as type 1.8s or 1.9s; they have relatively low intrinsic luminosities and, even if corrected for absorption, they would be bright Seyfert 1s or weak QSOs.

Fiore et al. (1999) have made a survey in the X-ray band 5-10 keV; the resulting sample contains 14 objects, 13 of which are associated with AGNs; one is a Liner, 6 are unreddened QSOs, while seven are Seyfert 1.8s or 1.9s; none are Seyfert 2s which is somewhat surprising since, in this X-ray band, objects with $N_H < 10^{24}$ cm^{-2} should not be affected by extinction and, as we have seen above, about half of all Seyfert 2s have such small column densities (Risaliti et al. 1999).

5.3. Type 2 QSOs

There have been several claims about the discovery of X-ray selected "narrow line" QSOs which have been called type 2 QSOs. All of them turned out to be normal broad line objects or, more often, NLS1s (which are difficult to distinguish from Seyfert 2s on low dispersion spectra) (Halpern & Moran 1998; Halpern et al. 1999).

Radio quiet type 2 QSOs should not look like QSOs at all, as both the non-thermal continuum and the broad emission lines should be completely suppressed by the obscuring torus, but rather as galaxies with high excitation narrow emission lines; such objects would not be optically conspicuous.

Radio loud type 2 QSOs however are relatively easy to find, since in low frequency surveys, the radio emission is dominated by the large radio lobes that are unaffected by any obscuration or beaming effects. The 3CR survey (Bennett 1962) is the best studied of all low frequency radio surveys; it covers the northern sky, including all point sources with flux density greater than 9.0 Jy at 178 MHz. From an analysis of the 3CR sources in the redshift range 0.5 $< z <$ 1.0, Barthel (1989) concluded that type 2 (*i.e.* NLRGs with a high radio luminosity) are twice as numerous as type 1 QSOs; however four of the narrow line objects in his sample (3C 22.0, 41.0, 265.0 and 325.0) are now known to have broad Balmer lines; the relative number of type 2 to type 1 QSOs then become 1.4:1. Lawrence (1991) carried out a similar analysis, and found that at high radio luminosities, the numbers of narrow and broad line objects are about equal.

Véron (1977) has built a new catalogue based on the 3CR at $|b| > 10°$, correcting the fluxes for confusion and resolution; it contains 205 extragalactic sources. The redshift of all of them except three (3C 89.0, 3C 249.0 and 4C−01.04) has been measured. This sample contains 17 objects having broad

emission lines and a radio luminosity larger than 10^{36} erg s^{-1} Hz^{-1}; 16 are QSOs ($M_B < -24$); it is reasonable to assume that all the 17 narrow line objects with such a high radio luminosity are type 2 QSOs, which leads to a ratio of type 2 to type 1 QSOs near one in the absolute magnitude range $-28 < M_B < -24$. This result is in good agreement with Lawrence (1991).

Stickel et al. (1996) have found 14 flat-spectrum radio sources with very weak optical-infrared counterparts and with very steep infrared-to-optical continua; many of them have narrow emission line spectra. Redshifted H I 21 cm absorption has been detected in four out of five of them, with neutral hydrogen column densities $\sim$ 4 and 80 10^{18} cm^{-2} suggesting that these objects are reddened by dust; the steep optical-infrared slopes suggest lower limits to rest-frame values of A_V between two and seven magnitudes; the location of the absorber, within or outside the host galaxy, is not known (Carilli et al. 1998). The corrected absolute magnitude of these objects could be brighter than $M_B = -24$ and therefore they could be type 2 QSOs.

From thermal-infrared (3.8 μm) imaging of 19 z$\sim$1 3C NLRGs, Simpson et al. (1999) determined that in $\sim$ 70% of these objects the nuclear extinction is $A_V > 15$ mag.

In the so-called receding torus model, the obscuring region has a constant physical thickness, but its inner edge is determined by the radius at which dust evaporates; this radius should be larger in more luminous objects, increasing as $L^{0.5}$; the general increase in UV luminosity with radio power will cause the opening angle of the obscuring torus to increase on average with radio luminosity and therefore the relative number of type 2 QSOs to decrease (Hill et al. 1996).

The obscuring torus present in AGNs is hiding the nuclear continuum and broad line region in type 2 objects; the waste heat from the torus appears in the IR, and while it may not scale exactly with luminosity if the torus opening angle is changing, it should still be conspicuous in type 2 QSOs. Dust emission in QSOs accounts for $\sim$ 30% of the luminosity in UV-selected QSOs (Sanders et al. 1989); if the torus is opaque and if it produces most of the FIR luminosity, then the torus covering factor is typically 30% and there should be twice as many type 1 as type 2 QSOs at a given value of an isotropic parameter such as FIR luminosity (Antonucci 1999); this is significantly larger than the observed ratio.

Three non-BALQSOs are known which show strong polarization of both the optical continuum and the broad emission lines: OI 287 (Goodrich & Miller 1988), WN J0717+4611 (de Breuck et al. 1998) and IRAS F10214+4724 (Goodrich et al. 1996). They have been interpreted as QSOs in which both the broad-line region and the continuum are completely obscured from direct view, being seen only by scattered radiation, the scattering producing a high degree of polarization of both the continuum and the broad emission lines. They could be considered as type 2 QSOs. 3C 68.1 is an intermediate case with both reddened scattered (polarized) QSO light diluted by even more dust-reddened QSO light reaching us directly from the nucleus (Brotherton et al. 1998).

6. CONCLUSIONS

We have reviewed a number of recent papers dealing with the most controversial aspects of AGNs. They suggest interesting conclusions:

-All Seyfert galaxies can be essentially described by a single parameter, the X-ray column density which steadily increases from Seyfert 1s to Seyfert 1.8s to Seyfert 1.9s to Seyfert 2s.

-AGNs belong to two main classes: the high-ionization AGNs (Seyfert 1s and 2s) and the low-ionization AGNs (Liners) which probably differ by the accretion rate onto the central BH, Liners having low accretion rates and consequently being powered by an unefficient advection dominated accretion flow.

-HPQs are high-ionization radio loud AGNs with a relativistic jet pointing in the direction of the observer, while BLLs are low-ionization AGNs. Many blazars have been classified as BLLs on the basis of unsufficient data; most objects with weak broad emission lines are HPQs.

-Radio loud AGNs may host a rapidly rotating BH, and radio quiet AGNs a slowly rotating BH. Rapidly spinning BHs could be the result of the merger of two similar mass BHs.

-Many early-type spirals have a nuclear emission line spectrum intermediate between Liners and starbursts (the so-called weak [O I]-Liners); they are probably old starbursts dominated by supernova remnants.

-Cooling flow clusters often show near their center a filamentary structure which has a Liner-like spectrum most probably ionized by stellar processes rather than by an AGN; on the other hand, the central galaxy in these clusters is often a FR I radio galaxy, *i.e.* a genuine AGN. The true nature of an emission line nebulosity observed in a FR I galaxy centrally located in a cooling flow cluster is therefore somewhat ambiguous.

-ULIGs are powered by starbursts induced by merging processes; many are weak [O I]-Liners. A significant fraction of all ULIGs contains an AGN which is probably the consequence of the merging; the AGN may, in some cases, be the major source of energy.

-Type 2 QSOs exist; they are in general quite inconspicuous as both the broad emission lines and the nuclear continuum are hidden from view. FR II radio galaxies with a high radio luminosity are type 2 QSOs.

Acknowledgement. We are pleased to thank Suzy Collin for constructive discussions and Areg Mickaelian for careful reading of the manuscript.

References

Abramowicz M.A., Calvani M., Madau P. 1987,Comments on astrophysics 12,67

Allen S.W. 1995,MNRAS 276,947
Allen S.W., Edge A.C., Fabian A.C. et al. 1992,MNRAS 259,67
Allen S.W., Fabian A.C. 1997,MNRAS 286,583
Allen S.W., Fabian A.C., Johnstone R.M., Arnaud K.A., Nulsen P.E.J. 1999, MNRAS (astro-ph/9910188)
Alonso-Herrero A., Rieke M.J., Rieke G.H., Shields J.C. 1999, ApJ (submitted) (astro-ph/9909316)
Antonucci R.R.J. 1993,ARA&A 31,473
Antonucci R.R.J. 1996,Vistas in astronomy 40,3
Antonucci R.R.J. 1999, (astro-ph/9811187)
Antonucci R.R.J., Miller J.S. 1985,ApJ 297,621
Antonucci R.R.J., Hickson P., Miller J.S., Olszewski E.W. 1987,AJ 93,785
Appl S., Camenzind M. 1993,in: Jets in extragalactic radio sources, Lecture notes in physics 421,123
Aretxaga I., Joguet B., Kunth D., Melnick J., Terlevich R.J. 1999,ApJ 519,L123
Bade N., Komossa S., Dahlem M. 1996,A&A 309,L35
Bahcall J.N., Kirhakos S., Saxe D.H., Schneider D.P. 1997,ApJ 479,642
Baker J.C. 1997,MNRAS 286,23
Baldwin J.A., Phillips M.M., Terlevich R. 1981,PASP 93,5
Ball R., Burns J.O., Loken C. 1993,AJ 105,53
Barnes J.E., Hernquist L. 1992,ARA&A 30,705
Barnes J.E. 1999,in: The evolution of galaxies on cosmological timescales, ASP Conf. Ser. (in press) (astro-ph/9903234)
Barth A.J., Reichert G.A., Filippenko A.V. et al. 1996,AJ 112,1829
Barth A.J., Reichert G.A., Ho L.C. et al. 1997,AJ 114,2313
Barth A.J., Ho L.C., Filippenko A.V., Sargent W.L.W. 1998,ApJ 496,133
Barth A.J., Filippenko A.V., Moran E.C. 1999a,ApJ 515,L61
Barth A.J., Filippenko A.V., Moran E.C. 1999b,ApJ (in press) (astro-ph/9905290)
Barthel P.D. 1989,ApJ 336,606
Bassani L., Dadina M., Maiolino R. et al. 1999,ApJS 121,473
Baum S.A., Zirbel E.L., O'Dea C. 1995,ApJ 451,88
Baum S.A., O'Dea C.P., Giovannini G. et al. 1997,ApJ 483,178
Begelman M.C. 1985,in: Astrophysics of active galaxies and quasi-stellar objects. J.S. Miller ed., Oxford University Press, p. 411
Begelman M.C., Blandford R.D., Rees M.J. 1980,Nat 287,307
Bekki K. 1999,ApJ Lett. (submitted) (astro-ph/9904044)
Bender R., Surma P., Döbereimer S., Möllenhoff C., Madejsky R. 1989,A&A 217,35
Benn C.R., Vigotti M., Carbalo R., González-Serrano J.I., Sanchez S.F. 1998, MNRAS 295,451
Bennett A.S. 1962,Mem. RAS 58,163
Bergeron J., Kunth D. 1984,MNRAS 207,263
Bertola F., Buson L.M., Zeilinger W.W. 1992,ApJ 401,L79
Bicknell G.V. 1994,ApJ 422,542
Bicknell G.V., de Ruiter H.R., Fanti R., Morganti R., Parma P. 1990,ApJ 354,98
Binette L. 1985,A&A 143,334
Binette L., Magris C.G., Stasinska G., Bruzual A.G. 1994,A&A 292,13
Binette L., Wilson A.S., Storchi-Bergmann T. 1996,A&A 312,365
Biretta J.A., Zhou F., Owen F.N. 1995,ApJ 447,582
Bischoff K., Kollatschny W. 1999,A&A 345,49
Blanco P.R., Ward M.J., Wright G.S. 1990,MNRAS 242,4P
Blandford R.D. 1990,in: Active galactic nuclei, Saas-Fee advanced course 20, T.J.-L. Courvoisier & M. Mayor eds., p. 161
Blandford R.D. 1994,ASP Conf. Ser. 54,23
Blandford R.D. 1999,ASP Conf. Ser. 160,265
Blandford R.D., Königl A. 1979,ApJ 232,34
Blundell K. M., Rawlings S., Willott C.J. 1999,AJ 117,677
Boller T., Trumper J., Molendi S. et al. 1993,A&A 279,53
Boller T., Brandt W.N., Fink H. 1996,A&A 305,53
Bonatto C.J., Pastoriza M.G. 1997,ApJ 486,132

Borne K.D., Bushouse H., Colina L. et al. 1999,Ap&SS (in press) (astro-ph/9902293)
Boroson T.A., Green R.F. 1992,ApJS 80,109
Boyce P.J., Disney M.J., Blades J.C. et al. 1998,MNRAS 298,121
Boyce P.J., Disney M.J., Bleaken D.G. 1999,MNRAS 302,L39
Braatz J.A., Wilson A.S., Henkel C. 1997,ApJS 106,51
Brandt W.N. 1999,ASP Conf.Ser. 161,166
Brandt W.N., Pounds K.A., Fink H. 1995,MNRAS 273,L47
Brandt W.N., Boller T., Fabian A.C., Ruszkowski M. 1999a,MNRAS 303,L53
Brandt W.N., Laor A., Wills B.J. 1999b,ApJ (in press) (astro-ph/9908016)
Bregman J.N. 1990,A&AR 2,125
Bridges T.J., Irwin J.A. 1998,MNRAS 300,967
Bridle A.H. 1984,AJ 89,979
Brotherton M.S., Wills B.J., Francis P.J., Steidel C.C. 1994,ApJ 430,495
Brotherton M.S., Wills B.J., Dey A., van Breugel W., Antonucci R. 1998,ApJ 501,110
Brown B.A., Bregman J.N. 1998,ApJ 495,L75
Burbidge G.R., Hewitt A. 1987,AJ 93,1
Burbidge G.R., Hewitt A. 1992, in: Variability of blazars, E. Valtaoja & M. Valtonen (eds), Cambridge university press, p. 4
Burbidge G.R., Jones T.W., O'Dell S.L. 1974,ApJ 193,43
Burns J.O. 1990,AJ 99,14
Capetti A., Celotti A. 1999,MNRAS 304,434
Cappi M., Bassani L., Comastri A. et al. 1999,A&A 344,857
Carilli C.L., Menten C.M., Reid M.J., Rupen M.P., Yun M.S. 1998,ApJ 494,175
Carrillo R., Cruz-Gonzalez I., Guichard J. 1999,Rev. Mex. A&A 35,45
Cassaro P., Stanghellini C., Bondi M. et al. 1999,A&A (in press) (astro-ph/9910209)
Catanese M., Weekes T.C. 1999,PASP (in press) (astro-ph/9906501)
Cattaneo A., Haehnelt M.G., Rees M.J. 1999,MNRAS 308,77
Chary R., Becklin E.E., Evans A.S. et al. 1999,ApJ 531 (astro-ph/9910557)
Chen K., Halpern J.P. 1989,ApJ 344,115
Chiaberge M., Capetti A., Celotti A. 1999,A&A 349,77
Claussen M.J., Diamond P.J., Braatz J.A., Wilson A.S., Henkel C. 1998,ApJ 500,L129
Cohen M.H., Ogle P.M., Tran H.D., Goodrich R.W., Miller J.S. 1999,AJ (in press) (astro-ph/9909215)
Cohen R.D. 1983,ApJ 273,489
Cohen R.D., Osterbrock D.E. 1981,ApJ 243,81
Colina L., de Juan L. 1995,ApJ 448,548
Collin-Souffrin S. 1987,A&A 179,60
Collin-Souffrin S. 1994,NATO ASI Series C 417,195
Collin-Souffrin S., Hameury J.-M., Joly M. 1988,A&A 205,19
Comastri A., Setti G., Zamorani G. et al. 1992,ApJ 384,62
Condon J.J., Huang Z.-P., Yin Q.F., Thuan T.X. 1991,ApJ 378,65
Corbett E.A., Robinson A., Axon D.J. et al. 1996,MNRAS 281,737
Corbin M.R. 1992,ApJ 391,577
Corbin M.R. 1995,ApJ 447,496
Côté P., Marzke R.O., West M.J. 1998,ApJ 501,554
Crawford C.S., Allen S.W., Ebeling H., Edge A.C., Fabian A.C. 1999, MNRAS 306,857
Crenshaw D.M. 1986,ApJS 62,821
Crenshaw D.M. 1997,ASP Conf. Ser. 113,240
de Breuck C., Brotherton M.S., Tran H.D., van Breugel W., Röttgering H.J.A. 1998,AJ 116,13
Deguchi S., Watson W.D. 1989,ApJ 340,L17
Di Matteo T., Fabian A.C. 1997,MNRAS 286,L50
Di Matteo T., Fabian A.C., Rees M.J., Carilli C.L., Ivison R.J. 1999,MNRAS 305,492
Donahue M., Stocke J.T., Gioia I.M. 1992,ApJ 385,49
Done C., Madejski G.M., Smith D.A. 1996,ApJ 463,L63
Downes D., Solomon P.M. 1998,ApJ 507,615
Dumont A.-M., Collin-Souffrin S., Nazarova L. 1998,A&A 331,11
Elvis M., Fiore F., Giommi P., Padovani P. 1998,ApJ 492,91
Eracleous M., Halpern J.P. 1994,ApJS 90,1

Erkens U., Appenzeller J., Wagner S. 1997,A&A 323,707
Evans A.S., Kim D.C., Mazzarella J.M., Scoville N.Z., Sanders D.B. 1999, ApJ 521,L107
Faber S.M., Tremaine S., Ajhar E.A. et al. 1997,AJ 114,1771
Fabian A.C. 1994,ARA&A 32,277
Fabian A.C., Canizares C.R. 1988,Nat 333,829
Fabian A.C., Rees M.J. 1995,MNRAS 277,L55
Fabian A.C., Arnaud K.A., Nulsen P.E.J., Mushotzky R.F. 1986,ApJ 305,9
Fanaroff B.L., Riley J.M. 1974,MNRAS 167,31P
Feldmeier J.J., Brandt W.N., Elvis M. et al. 1999,ApJ 510,167
Ferguson J.W., Korista K.T., Baldwin J.A., Ferland G.J. 1997a,ApJ 487,122
Ferguson J.W., Korista K.T., Ferland G.J. 1997b,ApJS 110,287
Fernini I., Burns J.O., Perley R.A. 1997,AJ 114,2292
Filippenko A.V. 1985,ApJ 289,475
Filippenko A.V. 1996,ASP Conf. Ser. 103,17
Filippenko A.V., Halpern J.P. 1984,ApJ 285,458
Filippenko A.V., Terlevich R. 1992,ApJ 397,L79
Fiore F., Laor A., Elvis M., Nicastro F., Giallongo E. 1998,ApJ 503,607
Fiore F., La Franca F., Giommi P. et al. 1999,MNRAS 306,L55
Forbes D.A. 1991,MNRAS 249,779
Forster K., Halpern J.P. 1996,ApJ 468,565
Franceschini A., Vercellone S., Fabian A.C. 1998,MNRAS 297,817
Francis P.J. 1993,ApJ 405,119
Francis P.J., Whiting M.T., Webster R.L. 1999,PASA (in press) (astro- ph/9911195)
Fujisawa K., Kobayashi H., Hirabayashi H. et al. 1999,PASJ 51,537
Gabuzda D.C., Mullan C.M., Cawthorne T.V., Wardle J.F.C., Roberts D.H. 1994, ApJ 435,140
Gallagher S.C., Brandt W.N., Sambruna R.M., Mathur S., Yamasaki N. 1999, ApJ 519,549
Gallimore J.F., Baum S.A., O'Dea C.P., Brinks E., Pedlar A. 1996,ApJ 462,740
Gammie C.F., Narayan R., Blanford R.D. 1999,ApJ 516,177
Garrington S.T., Conway R.G. 1991,MNRAS 250,198
Genzel R., Lutz D., Sturm E. et al. 1998,ApJ 498,579
Georgantopoulos I., Almaini O., Shanks T. et al. 1999,MNRAS 305,125
George I.M., Turner T.J., Netzer H. et al. 1998a,ApJS 114,73
George I.M., Turner T.J., Mushotzky R., Nandra K., Netzer H. 1998b,ApJ 503,174
Ghisellini G., Padovani P., Celotti A., Maraschi L. 1993,ApJ 407,65
Giommi P., Ansari S.G., Micol A. 1995,A&AS 109,267
Giovannini G., Feretti L., Venturi T. et al. 1994,ApJ 435,116
Giovannini G., Cotton W.D., Lara L., Venturi T. 1996,IAU Symp. 175,127
Giovannini G., Taylor G.B., Arbizzani E. et al. 1999,ApJ 522,101
Goldader J.G., Joseph R.D., Doyon R., Sanders D.B. 1995,ApJ 444,97
Gomez P.L., Pinkney J., Burns J.O. et al. 1997,ApJ 474,580
Gonçalves A.C., Véron P., Véron-Cetty M.-P., 1998,A&A 333,877
Gonçalves A.C., Véron-Cetty M.-P., Véron P. 1999,A&AS 135,437
Gondhalekar P.M., Rouillon-Foley C., Kellett B.J. 1997,MNRAS 288,260
González-Serrano J.I., Carballo R., Pérez-Fournon I. 1993,AJ 105,1710
Goodrich R.W. 1989a,ApJ 340,190
Goodrich R.W. 1989b,ApJ 342,224
Goodrich R.W. 1990,ApJ 355,88
Goodrich R.W. 1995,ApJ 440,141
Goodrich R.W., Miller J.S. 1988,ApJ 331,332
Goodrich R.W., Veilleux S., Hill G.J. 1994,ApJ 422,521
Goodrich R.W., Miller J.S., Martel A. et al. 1996,ApJ 456,L9
Gopal-Krishna G., Biermann L. 1998,A&A 330,L37
Goudfrooij P. 1999,ASP Conf. Ser. 163,55
Goudfrooij P., de Jong T. 1995,A&A 298,784
Goudfrooij P., Hansen L., Jørgensen H.E., Nørgaard-Nielsen H.U., 1994,A&AS 105,341
Granato G.L., Danese L., Franceschini A. 1997,ApJ 486,147
Grandi S.A. 1981,ApJ 251,451
Grandi S.A., Osterbrock D.E. 1978,ApJ 220,783

Greenhill L.J., Jiang D.R., Moran J.M. et al. 1995,ApJ 440,619
Grupe D., Beuerman K., Mannheim K. et al. 1995a,A&A 299,L5
Grupe D., Beuerman K., Mannheim K. et al. 1995b,A&A 300,L21
Grupe D., Wills B.J., Wills D., Beuermann K. 1998,A&A 333,827
Grupe D., Beuermann K., Mannheim K., Thomas H.-C. 1999a,A&A 350,805
Grupe D., Thomas H.-C., Leighly K.M. 1999b,A&A 350,L31
Guainazzi M., Antonelli L.A. 1999,MNRAS 304,L15
Guainazzi M., Nicastro F., Fiore F. et al. 1998,MNRAS 301,L1
Guainazzi M., Matt G., Molendi S. et al. 1999,A&A 341,L27
Güijosa A., Daly R.A. 1996,ApJ 461,600
Halpern J.P., Filippenko A.V. 1984,ApJ 285,475
Halpern J.P., Eracleous M. 1994,ApJ 433,L17
Halpern J.P., Moran E.C. 1998,ApJ 494,194
Halpern J.P., Helfand D.J., Moran E.C. 1995,ApJ 453,611
Halpern J.P., Turner T.J., George I.M. 1999,MNRAS 307,L47
Hardcastle M.J., Worrall D.M. 1999,MNRAS 309,969
Hardcastle M.J., Alexander P., Pooley G.G., Riley J.M. 1998, MNRAS 296,445
Hardcastle M.J., Alexander P., Pooley G.G., Riley J.M. 1999, MNRAS 304,135
Heckman T.M. 1980,A&A 87,152
Heckman T.M. 1987,IAU Symp. 121,421
Heidt J., Wagner S.J. 1996,A&A 305,42
Heisler C.A., Lumsden S.L., Balley J.A. 1997,Nat 385,700
Helou G., Soifer B.T., Rowan-Robinson M. 1985,ApJ 298,L7
Herrstein J.R., Greenhill L.J., Moran J.M. et al. 1998,ApJ 497,L69
Hill G.J., Lilly S.J. 1991,ApJ 367,1
Hill G.J., Goodrich R.W., DePoy D.L. 1996,ApJ 462,163
Ho L.C. 1998,in: The AGN-galaxy connection. 32nd COSPAR meeting. Advances in space research (in press) (astro-ph/9807273)
Ho L.C., Filippenko A.V., Sargent W.L.W. 1993a,ApJ 417,63
Ho L.C., Shields J.C., Filippenko A.V. 1993b,ApJ 410,567
Ho L.C., Filippenko A.V., Sargent W.L.W. 1997a,ApJ 487,568
Ho L.C., Filippenko A.V., Sargent W.L.W., Peng C.Y. 1997b,ApJS 112,391
Ho L.C., Filippenko A.V., Sargent W.L.W., Peng C.Y. 1997c,ApJS 112,315
Huchra J.P., Burg R. 1992,ApJ 393,90
Hughes P.A., Aller H.D., Aller M.F. 1992,ApJ 396,469
Imanishi M., Ueno S. 1999,MNRAS 305,829
Iwasawa K., Koyama K., Awaki H. et al. 1993,ApJ 409,155
Iwasawa K., Fabian A.C., Young A.J., Inoue H., Matsumoto C. 1999,MNRAS 306,L19
Jackson C.A., Wall J.V. 1999,MNRAS 304,160
Jackson N., Browne I.W.A. 1991,MNRAS 250,422
Jackson N., Rawlings S. 1997,MNRAS 286,241
Jaffe W., Bremer M.N. 1997,MNRAS 284,L1
Joly M. 1981,A&A 102,321
Joly M. 1987,A&A 184,33
Joly M. 1991,A&A 242,49
Jones P.A., McAdam W.B. 1992,ApJS 80,137
Joseph R.D. 1999,A&SS (in press) (preprint IfA-99-30)
Joseph R.D., Wright G.S. 1985,MNRAS 214,87
Kartje J.F., Königl A., Elitzur M. 1999,ApJ 513,180
Kaspi S., Smith P.S., Maoz D., Netzer H., Jannuzi B.T. 1996,ApJ 471,L75
Kellermann K.I., Vermeulen R.C., Zensus J.A., Cohen M.H. 1998,AJ 115,1295
Kim D.-W. 1989,ApJ 346,653
Kim D.-W., Elvis M. 1999,ApJ 516,9
Kissler-Patig M., Forbes D.A., Minniti D. 1998,MNRAS 298,1123
Knapp G.R., Turner E.L., Cunniffe P.E. 1985,AJ 90,454
Kollgaard R.I. 1994,Vistas in Astronomy 38,29
Kollgaard R.I., Palma C., Laurent-Muehleisen S.A., Feigelson E.D. 1996, ApJ 465,115
Komossa S., Schulz H. 1997,A&A 323,31

Komossa S., Schulz H. 1998,A&A 339,345
Komossa S., Bade N. 1999,A&A 343,775
Komossa S., Greiner J. 1999,A&A 349,L45
Komossa S., Böhringer H., Huchra J.P. 1999,A&A 349,88
Koratkar A., Blaes O. 1999,PASP 111,1
Koratkar A., Deustua S.E., Heckman T. et al. 1995,ApJ 440,132
Korista K. 1999,ASP Conf. Ser. 162,165
Kormendy J., Richstone D. 1995,ARA&A 33,581
Kormendy J., Bender R. 1996,ApJ 464,L119
Koski A.T. 1978,ApJ 223,56
Koski A.T., Osterbrock D.E. 1976,ApJ 203,L49
Kotilainen J.K., Falomo R., Scarpa R. 1998,A&A 336,479
Krolik J.H., Kallman T.R. 1987,ApJ 320,L5
Kwan J., Cheng F.-Z., Fang L.-Z., Zheng W., Ge J. 1995,ApJ 440,628
Lähteenmäki A., Valtaoja E. 1999,ApJ 521,493
Lähteenmäki A., Valtaoja E., Wiik K. 1999,ApJ 511,112
Laing R.A. 1988,Nat 331,149
Laing R.A., Jenkins C.R., Wall J.V., Unger S.W. 1994,ASP Conf. Ser. 54,201
Laing R.A., Parma P., de Ruiter H.R., Fanti R. 1999,MNRAS 306,513
Laor A. 1998,ApJ 505,L83
Laor A., Fiore F., Elvis M., Wilkes B.J., McDowell J.C. 1994,ApJ 435,611
Laor A., Fiore F., Elvis M., Wilkes B.J., McDowell J.C. 1997a,ApJ 477,93
Laor A., Jannuzi B.T., Green R.F., Boroson T.A. 1997b,ApJ 489,656
Lara L., Cotton W.D., Feretti L. et al. 1997,ApJ 474,179
Lara L., Marquez I., Cotton W.D. et al. 1999,New Astron. Rev. (astro-ph/9812254)
Lasota J.-P., Abramowicz M.A., Chen X. et al. 1996,ApJ 462,142
Laurent-Muehleisen S.A., Kollgaard R.I., Feigelson E.D., Brinkmann W., Siebert J. 1999,ApJ (in press) (astro-ph/9905133)
Lawrence A. 1987,PASP 99,309
Lawrence A. 1991,MNRAS 252,586
Lawrence A., Walker D., Rowan-Robinson M., Leech K.J., Penston M.V. 1986,MNRAS 219,687
Lawrence A., Saunders W., Rowan-Robinson M. et al. 1988,MNRAS 235,261
Lawrence A., Elvis M., Wilkes B.J., M^{c}Hardy I., Brandt N. 1997, MNRAS 285,879
Ledlow M.J., Owen F.N. 1995,AJ 110,1959
Ledlow M.J., Owen F.N. 1996,AJ 112,9
Ledlow M.J., Owen F.N., Keel W.C. 1999,IAU Symp. 186,359
Lehnert M.D., Miley G.K., Sparks W.B. et al. 1999,ApJS 123,351
Leighly K.M. 1999a,ApJS (in press) (astro-ph/9907294)
Leighly K.M. 1999b,ApJS (in press) (astro-ph/9907295)
Leighly K.M., Kay L.E., Wills B.J., Wills D., Grupe D. 1997,ApJ 489,L137
Lightman A.P., White T.R. 1988,ApJ 335,57
Lilly S.J., Prestage R.M. 1987,MNRAS 225,531
Lipari S. 1994,ApJ 436,102
Lipari S., Terlevich R., Macchetto F. 1993,ApJ 406,451
Lutz D., Spoon H.W.W., Rigopoulou D., Moorwood A.F.M., Genzel R. 1998,ApJ 505,L103
Lutz D., Veilleux S., Genzel R. 1999,ApJ 517,L13
Macchetto F., Pastoriza M., Caon N. et al. 1996,A&AS 120,463
Mack K.-H., Klein U., O'Dea C.P., Willis A.G. 1997,A&AS 123,423
Magdziarz P., Zdziarski A.A. 1995,A&A 273,837
Magorrian J., Tremaine S., Richstone D. et al. 1998,AJ 115,2285
Mahadevan R. 1997,ApJ 477,585
Mahadevan R. 1999,MNRAS 304,501
Maiolino R., Rieke G.H. 1995,ApJ 454,95
Maiolino R., Salvati M., Bassani L. et al. 1998,A&A 338,781
Malizia A., Bassani L., Stephen J.B., Malaguti G., Palumbo G.G.C. 1997,ApJS 113,311
Malkan M.A., Gorjian V., Tam R. 1998,ApJS 117,25
Maoz D., Koratkar A., Shields J.C. et al. 1998,AJ 116,55
Maraschi L., Rovetti F. 1994,ApJ 436,79

Martel A.R., Baum S.A., Sparks W.B. et al. 1999,ApJS 122,81
Masci F.J., Webster R.L., Francis P.J. 1998,MNRAS 301,975
Mathur S., Wilkes B., Elvis M. 1998,ApJ 503,L23
Matt G. 1997,Mem. Soc. Astron. Ital. 68,127
Matt G., Perola G.C., Piro L. 1991,A&A 247,25
M^{c}Hardy I.M., Merrifield M.R., Abraham R.G., Crawford C.S. 1994,MNRAS 268.681
McIntosh D.H., Rieke M.J., Rix H.-W., Foltz C.B., Weyman R.J. 1999,ApJ 514,40
McLure R.J., Kukula M.J., Dunlop J.S. et al. 1999,MNRAS 308,377
Meier D.L. 1999,in: Life cycles of radio galaxies, eds. Biretta et al., New Astronomy Reviews (in press) (astro-ph/9908283)
Merritt D. 1993,Science 259,1867
Miley G.K. 1980,ARA&A 18,165
Miller P., Rawlings S., Saunders R., Eales S. 1992,MNRAS 254,93
Mirabel I.F., Wilson A.S. 1984,ApJ 277,92
Miyoshi M., Moran J., Herrstein J. et al. 1995,Nat 373,127
Möllenbrock G.A., Fujisawa K., Preston R.A. et al. 1996,AJ 111,2174
Molthagen K., Bade N., Wendker H.J. 1998,A&A 331,925
Moran A.C., Halpern J.P., Helfand D.J. 1996,ApJS 106,341
Morganti R., Killeen N.E.B., Tadhunter C.N. 1993,MNRAS 263,1023
Morganti R., Oosterloo T.A., Fosbury R.A.E., Tadhunter C.N. 1995,MNRAS 274,393
Morganti R., Oosterloo T.A., Reynolds J.E., Tadhunter C.N., Migenes V. 1997,MNRAS 284,541
Morris S.L., Ward M.J. 1985,MNRAS 215,57P
Morris S.L., Stocke J.T., Gioia I.M. et al. 1991,ApJ 380,49
Morrison R., McCammon D. 1983,ApJ 270,119
Mukherjee R., Bertsch D.L., Bloom S.D. et al. 1997,ApJ 490,116
Mulchaey J.S., Mushotzky R.F., Weaver K.A. 1992,ApJ 390,L69
Murphy T.W., Soifer B.T., Matthews K., Kiger J.R., Armus L. 1999,ApJ (in press) (astro-ph/9909245)
Mushotzky R.F. 1982,ApJ 256,92
Mushotzky R.F. 1997,ASP Conf. Ser. 128,141
Mushotzky R.F., Done C., Pounds K.A. 1993,ARA&A 31,717
Naab T., Burkert A., Hernquist L. 1999,ApJ 523,L133
Nandra K., Pounds K.A. 1994,MNRAS 268,405
Nandra K., George I.M., Mushotzky R.F., Turner T.J., Yaqoob T. 1997a,ApJ 476,70
Nandra K., George I.M., Mushotzky R.F., Turner T.J., Yaqoob T. 1997b,ApJ 477,602
Nandra K., George I.M., Mushotzky R.F., Turner T.J., Yaqoob T. 1999,ApJ 523,L17
Narayan R., Mahadevan R., Quataert E. 1999,in: The theory of black hole accretion disks, eds. M.A. Abramowicz, G. Bjornsson & J.E. Pringle (Cambridge University Press) (astro-ph/9803141)
Nelson C.H., Whittle M. 1996,ApJ 465,96
Netzer H. 1990,in: Active galactic nuclei, Saas-Fee advanced course 20, T.J.-L. Courvoisier & M. Mayor eds., p. 57
Nieto J.-L., Bender R. 1989,A&A 215,266
Ogle P.M., Cohen M.H., Miller J.S. et al. 1999, ApJS (astro-ph/9905299)
Oliva E., Origlia L., Maiolino R., Moorwood A.F.M. 1999,A&A (in press) (astro-ph/9908063)
Osterbrock D.E. 1977,ApJ 215,733
Osterbrock D.E. 1981,ApJ 249,462
Osterbrock D.E. 1987,in: Active galactic nuclei, Lecture notes in physics 307,1
Osterbrock D.E., Pogge R.W. 1985,ApJ 297,166
Osterbrock D.E., Mathews W.G. 1986,ARA&A 24,171
Osterbrock D.E., Shaw R.A. 1988,ApJ 327,89
Osterbrock D.E., Tran H.D., Veilleux S. 1992,ApJ 389,196
Owen F.N., Laing R.A. 1989,MNRAS 238,357
Owen F.N., Ledlow M.J., Keel W.C. 1996,AJ 111,53
Padovani P. 1992,A&A 256,399
Pearson T.J. 1996,ASP Conf. Ser. 100,97
Peres C.B., Fabian A.C., Edge A.C. et al. 1998,MNRAS 298,416

Perlman E.S., Stocke J.T. 1993,ApJ 406,430
Perlman E.S., Padovani P., Giommi P. et al. 1998,AJ 115,1253
Phillips M.M., Charles P.A., Baldwin J.A. 1983,ApJ 266,485
Piner B.G., Unwin S.C., Wehrle A.E. et al. 1999,ApJ (in press) (astro-ph/9906202)
Piro L., Matt G., Ricci R. 1997,A&AS 126,525 ApJS 106,399
Pounds K.A., Done C., Osborne J.P. 1995,MNRAS 277,L5
Predehl P., Schmitt J.H.M.M. 1995,A&A 293,889
Ptak A., Yaqoob T., Mushotzky R., Serlemitsos P.J., Griffiths R. 1998, ApJ 501,L37
Puchnarewicz E.M., Mason K.O., Cordova F.A. et al. 1992,MNRAS 256,589
Puchnarewicz E.M., Mason K.O., Carrera F.J. et al. 1997,MNRAS 291,177
Rawlings S., Lacy M., Sivia D.S., Eales S.A. 1995,MNRAS 274,428
Readhead A.C.S. 1994,ApJ 426,51
Rees M.J., Begelman M.C., Blandford R.D., Phinney E.S. 1982,Nat 295,17
Reynolds C.S. 1997,MNRAS 286,513
Reynolds C.S., Di Matteo T., Fabian A.C., Hwang U., Canizares C.R. 1996,MNRAS 283,L111
Reynolds C.S., Ward M.J., Fabian A.C., Celotti A. 1997,MNRAS 291,403
Richstone D., Ajhar E.A., Bender R. et al. 1998,Nat 395,A14
Rigopoulou D., Lawrence A., Rowan-Robinson M. 1996,MNRAS 278,1049
Rigopoulou D., Spoon H.W.W., Genzel R. et al. 1999,AJ (in press) (astro-ph/9908300)
Risaliti G., Maiolino R., Salvati M. 1999,ApJ 522,157
Rix H.-W., Carleton N.P., Rieke G., Rieke M. 1990,ApJ 363,480
Rodriguez-Ardila A., Pastoriza M.G., Bica E., Maza J. 1996,ApJ 463,522
Rodriguez Espinosa J.M., Rudy R.J., Jones B. 1987,ApJ 312,555
Rodriguez-Pascual P.M., Mas-Hesse J.M., Santos-Lleo M. 1997,A&A 327,72
Rokaki E., Boisson C., Collin-Souffrin S. 1992,A&A 253,57
Roos N., Kaastra J.S., Hummel C.AS. 1993,ApJ 409,130
Rowan-Robinson M. 1995,MNRAS 272,737
Rowan-Robinson M., Efstathiou A. 1993,MNRAS 263,675
Ruiz M., Rieke G.H., Schmidt G.D. 1994,ApJ 423,608
Sadler E.M., Jenkins C.R., Kotanyi C.G. 1989,MNRAS 240,591
Saikia D.J., Salter C.J. 1988,ARA&A 26,93
Sambruna R.M., Eracleous M., Mushotzky R.F. 1999,ApJ (in press) (astro-ph/9905365)
Sanders D.B. 1999,A&SS (in press) (astro-ph/9908297)
Sanders D.B., Mirabel I.F. 1996,ARA&A 34,749
Sanders D.B., Phinney E.S., Neugebauer G., Soifer B.T., Matthews K. 1989, ApJ 347,29
Sarazin C.L., McNamara B.R. 1997,ApJ 480,203
Scarpa R., Falomo R. 1997,A&A 325,109
Scarpa R., Urry C.M., Falomo R., Pesce J.E., Treves A. 1999,ApJS (in press) (astro-ph/9911147)
Scheuer P.A.G. 1992,in: Extragalactic radio sources. From beams to jets. J. Roland, H. Sol & G. Pelletier (eds.). Cambridge university press, p 368
Scheuer P.A.G. 1993,in: Jets in extragalactic radio sources, Lecture notes in physics 421,293
Schmidt G.D., Hines D.C. 1999,ApJ 512,125
Schmitt H.R. 1998,ApJ 506,647
Schnopper H.W., Davis M., Delvaille J.P., Geller M.J., Huchra J.P. 1978, Nat 275,719
Shanks T., Almaini O., Boyle B.J. et al. 1996,MPE Report 263,341
Shields G.A. 1999,PASP 111,661
Shields J.C. 1992,ApJ 399,L27
Shier L.M., Fisher J. 1998,ApJ 497,163
Shuder J.M. 1980,ApJ 240,32
Siebert J., Leighly K.M., Laurent-Muehleisen S.A. et al. 1999,A&A 348,678
Sikora M. 1994,ApJS 90,923
Sillanpää A. 1999,in: Observational evidence for black holes in the universe, S.K. Chakrabarti ed., Astrophysics and space science library (in press)
Sillanpää A., Takalo L.O., Pursimo T. et al. 1996,A&A 315,L13
Simkin S.M., Su H.J., Schwarz M.P. 1980,ApJ 237,404
Simpson C. 1998,MNRAS 297,L39
Simpson C., Ward M., Clements D.L., Rawlings S. 1996,MNRAS 281,509

Simpson C., Rawlings S., Lacy M. 1999,MNRAS 306,828
Singh K.P. 1999,MNRAS 309,991
Slee O.B., Sadler E., Reynolds J.E., Ekers R.D. 1994,MNRAS 269,928
Smith A.G., Nair A.D. 1995,PASP 107,863
Smith D.A., Done C. 1996,MNRAS 280,355
Smith E.P., Heckman T.M. 1989,ApJ 341,658
Smith E.P., Bohlin R.C., Bothun G.D. et al. 1997,ApJ 478,516
Soifer B.T., Houck J.R., Neugebauer G. 1987,ARA&A 25,187
Soifer B.T., Neugebauer G., Matthews K. et al. 1999,AJ (in press) (astro-ph/9911045)
Sopp H.M., Alexander P. 1992,MNRAS 259,425
Steidel C.S., Sargent W.L.W. 1991,ApJ 382,433
Stickel M., Padovani P., Urry C.M., Kühr H. 1991,ApJ 374,431
Stickel M., Rieke G.H., Kuhr H., Rieke M.J. 1996,ApJ 468,556
Stirpe G.M. 1991,A&A 247,3
Stocke J.T., Morris S.L., Gioia I.M. et al. 1991,ApJS 76,813
Stocke J.T., Wurtz R., Wang Q., Elston R., Januzzi B.T. 1992,ApJ 400,L17
Storchi-Bergmann T., Eracleous M., Livio M. et al. 1995,ApJ 443,617
Sulentic J.W., Marziani P., Zwitter T., Calvani M., Dultzin-Hacyan D. 1998,ApJ 501,54
Sundelius B., Wahde M., Lehto H.J., Valtonen M.J. 1997,ApJ 484,180
Surace J.A., Sanders D.B. 1999,ApJ 512,162
Surace J.A., Sanders D.B., Evans A.S. 1999,ApJ (in press) (astro-ph/9909085)
Tadhunter C.N., Morganti R., Robinson A. et al. 1998,MNRAS 298,1035
Takalo L.O. 1994,Vistas in Astronomy 38,77
Taniguchi Y., Yoshino A., Ohyama Y., Nishiura S. 1999,ApJ 514,660
Terashima Y., Ho L.C., Ptak A.F., Kunieda H. 1999,ApJ (in press) (astro-ph/9911340)
Thomas P.A., Fabian A.C., Arnaud K.A., Forman W., Jones J. 1986,MNRAS 222,655
Toomre A., Toomre J. 1972,ApJ 178,623
Tran H.D., Osterbrock D.E., Martel A. 1992,AJ 104,2072
Tran H.D., Marshall M.H., Goodrich R.W. 1995,AJ 110,2597
Tran H.D., Brotherton M.S., Stanford S.A. et al. 1999,ApJ 516,85
Trussoni E., Massaglia S., Ferrari R. et al. 1997,A&A 327,27
Trussoni E., Vagnetti F., Massaglia S. et al. 1999,A&A 348,437
Turner T.J., Pounds K.A. 1988,MNRAS 232,463
Turner T.J., Pounds K.A. 1989,MNRAS 240,833
Turner T.J., George I.M., Nandra K., Mushotzky R.F. 1997a,ApJS 113,23
Turner T.J., George I.M., Nandra K., Mushotzky R.F. 1997b,ApJ 488,164
Turner T.J., George I.M., Nandra K., Turcan D. 1999a,ApJ 524,667
Turner T.J., Perola G.C., Fiore F. et al. 1999b,ApJ 531 (astro-ph/9910216)
Turnshek D.A. 1995, in: QSO absorption lines, G. Meylan ed., ESO astrophysical symposium, p. 223
Turnshek D.A., Monier E.M., Sirola C.J., Espey B.R. 1997,ApJ 476,40
Ueno S., Law-Green J.D., Awaki H., Koyama K. 1998,IAU Symp. 188,432
Ulrich M.-H., Maraschi L., Urry C.M. 1997,ARA&A 35,445
Urry C.M., Padovani P. 1995,PASP 107,803
Urry C.M., Padovani P., Stickel M. 1991,ApJ 382,501
Urry C.M., Falomo R., Scarpa R. et al. 1999,ApJ 512,88
Valtaoja E., Teräsranta H., Lainela M., Teerikorpi P. 1992, in: Variability of blazars, E. Valtaoja & M. Valtonen (eds), Cambridge University Press, p 70
van der Marel R.P. 1999,AJ 117,744
Vaughan S., Reeves J., Warwick R., Edelson R. 1999a,MNRAS (in press) (astro-ph/9905323)
Vaughan S., Pounds K.A., Reeves J., Warwick R., Edelson R. 1999b,MNRAS (submitted) (astro-ph/9906445)
Veilleux S., Osterbrock D.E. 1987,ApJS 63,295
Veilleux S., Goodrich R.W., Hill G.J. 1997a,ApJ 477,631
Veilleux S., Sanders D.B., Kim D.-C. 1997,ApJ 484,92
Veilleux S., Sanders D.B., Kim D.-C. 1999,ApJ 522,139
Venturi T., Castaldini C., Cotton W.D. et al. 1995,ApJ 454,735
Vermeulen R.C., Cohen M.H. 1994,ApJ 430,467

Verner E.M., Verner D.A., Korista K.T. et al. 1999,A&AS 120,101
Véron P. 1977,A&AS 30,131
Véron P., Véron-Cetty M.-P. 1986,A&A 161,145
Véron P., Véron-Cetty M.-P. 1995,A&A 296,315
Véron P., Lindblad P.O., Zuidewijk E.J., Véron M.-P., Adam G. 1980,A&A 87,245
Véron-Cetty M.-P., Woltjer L. 1990,A&A 236,69
Viegas S.M., Contini M., Contini T. 1999,A&A 347,112
Vignati P., Molendi S., Matt G. et al. 1999,A&A 349,L57
Villata M., Raiteri C.M., Sillanpää A., Takalo L.O. 1998,MNRAS 293,L13
Voit G.M., Donahue M. 1997,ApJ 486,242
Wagner S.J., Witzel A. 1995,ARA&A 33,163
Wall J.V., Jackson C.A. 1997,MNRAS 290,L17
Wallinder F.H., Kato S., Abramowicz M.A. 1992,A&AR 4,79
Walter R., Fink H.H. 1993,A&A 274,105
Walter R., Orr A., Courvoisier T. J.-L. 1994,A&A 285,119
Wandel A. 1997,ApJ 490,L131
Wandel A. 1999,ApJ 519,L39
Wandel A., Peterson B.M., Malkan M.A. 1999,ApJ (in press) (astro-ph/9905224)
Wang J.X., Zhou Y.Y., Xu H.G., Wang T.G. 1999a,ApJ 516,L65
Wang T., Brinkmann W., Bergeron J. 1996,A&A 309,81
Wang T.G., Brinkmann W., Wamsteker W., Yuan W., Wang J.X. 1999b,MNRAS 307,821
Ward M.J., Wilson A.S., Penston M.V. et al. 1978,ApJ 223,788
Wardle J.F.C., Aaron S.E. 1997,MNRAS 286,425
Warwick R.S., Koyama K., Inoue H. et al. 1989,PASJ 41,739
Warwick R.S., Sembay S., Yaqoob T. et al. 1993,MNRAS 265,412
Weaver K.A., Wilson A.S., Henkel C., Braatz J.A. 1999,ApJ 520,130
Webster R.L., Francis P.J., Peterson B.A., Drinkwater M.J., Masci F.J. 1995,Nat 375,469
Weymann R.J. 1997,ASP Conf. Ser. 128,3
Weymann R.J., Morris S.L., Foltz C.B., Hewett P.C. 1991,ApJ 373,23
Willott C.J., Rawlings S., Blundell K.M., Lacy M. 1998,MNRAS 300,625
Willott C.J., Rawlings S., Blundell K.M., Lacy M. 1999,MNRAS (in press) (astro-ph/9905388)
Wills B.J. 1999,ASP Conf. Ser. 162,101
Wills B.J., Browne I.W.A. 1986,ApJ 302,56
Wills B.J., Netzer H., Wills D. 1985,ApJ 288,94
Wilman R.J., Fabian A.C., Cutri R.M. et al. 1998,MNRAS 300, L7
Wilson A.S., Colbert E.J.M. 1995,ApJ 438,62
Woltjer L. 1959,ApJ 130,38
Wozniak P., Zdziarski A.A., Smith D., Madejski G.M., Johnson W.N. 1998,MNRAS 299,449
Wu H., Zou Z.L., Xia X.Y., Deng Z.G. 1998,A&AS 132,181
Xu C., Livio M., Baum S. 1999,AJ 118,1169
Xue S.-J., Otani C., Mihara T., Cappi M., Matsuoka M. 1998,PASJ 50,519
Yi I., Boughn S.P. 1999,ApJ 515,576
Young S., Hough J.H., Axon D.J., Ward M.J., Bailey J.A. 1996a,MNRAS 280,291
Young S., Hough J.H., Efstathiou A. et al. 1996b,MNRAS 281,1206
Young S., Axon D.J., Hough J.H., Fabian A.C., Ward M.J. 1998,MNRAS 294,478
Yuan W., Brinkmann W., Siebert J., Voges W. 1998,A&A 330,108
Zensus J.A. 1997,ARA&A 35,607
Zheng W., Keel W.C. 1991,ApJ 382,121
Zirbel E.L. 1996,ApJ 473,713
Zirbel E.L. 1997,ApJ 476,489
Zirbel E.L., Baum S.A. 1995,ApJ 448,521

This article was processed by the author using the LaTeX style file *pljour1* from Springer-Verlag.

Table 6. List of the acronyms used

ADAF	Advection Dominated Accretion Flow
AGN	Active Galactic Nuclei
BAL	Broad Absorption Line
BALQSO	Broad Absorption Line QSO
BH	Black Hole
BLL	BL Lacertae object
BLR	broad line region
BLRG	Broad Line Radio Galaxy
BLS1	Broad Line Seyfert 1
FIR	Far-InfraRed
FR I	Fanaroff-Riley type I
FR II	Fanaroff-Riley type II
FWHM	Full Width at Half Maximum
gE	giant Elliptical galaxy
HBL	High energy peaked BLL
HPQ	Highly Polarized Quasar
HST	Hubble Space Telescope
HX	Hard X-ray (2-10 keV)
ILR	Intermediate Line Region
IRAS	InfraRed Astronomical Satellite
LBL	Low energy peaked BLL
LERG	Low-Excitation Radio Galaxy
Liner	Low Ionization Nuclear Emission line Region
L_X	X-ray Luminosity
M_B	Blue absolute magnitude
M_R	Red absolute magnitude
MIR	Mid-InfraRed
NELG	Narrow Emission Line X-ray Galaxy (=NLXG)
NLR	Narrow Line Region
NLRG	Narrow Line Radio Galaxy
NLS1	Narrow Line Seyfert 1
NLXG	Narrow emission Line X-ray Galaxy
PAH	Polycyclic Aromatic Hydrocarbon
QSO	Quasi Stellar Object or quasar
R	Flux ratio of the core to the extended radio components
R_S	Schwarzschild radius: $2GM/c^2$
RBL	Radio selected BLL
ROSAT	Röntgen Observatory SATellite
SMBBH	SuperMassive Binary Black Hole
SNR	SuperNova Remnant
S1h	Seyfert 1 galaxy with a hidden BLR
S1i	Seyfert 1 galaxy with an absorbed BLR visible in infrared
ULIG	UltraLuminous Infrared Galaxy
VBLR	Very Broad Line Region
XBL	X-ray selected BLL